

RESEARCH PAPER

Dynamic regulation of anthocyanin biosynthesis at different light intensities by the BT2-TCP46-MYB1 module in apple

Jian-Ping An, Ya-Jing Liu, Xiao-Wei Zhang, Si-Qi Bi, Xiao-Fei Wang, Chun-Xiang You and Yu-Jin Hao^{*} 

State Key Laboratory of Crop Biology, Shandong Collaborative Innovation Center for Fruit and Vegetable Production with High Quality and Efficiency, College of Horticulture Science and Engineering, Shandong Agricultural University, Tai-An, 271018, Shandong, China

* Correspondence: haoyujin@sdau.edu.cn

Received 4 November 2019; Editorial decision 14 January 2020; Accepted 29 January 2020

Editor: Ariel Vicente, CONICET- National University of La Plata, Argentina

Abstract

Teosinte branched1/cycloidea/proliferating (TCP) transcription factors play a broad role in plant growth and development, but their involvement in the regulation of anthocyanin biosynthesis is currently unclear. In this study, anthocyanin biosynthesis induced by different light intensities in apple (*Malus domestica*) was found to be largely dependent on the functions of the MdMYB1 and MdTCP46 transcription factors. The expression of MdTCP46 was responsive to high light intensity, and under these conditions it promoted anthocyanin biosynthesis by direct interactions with MdMYB1 that enhanced the binding of the latter to its target genes. MdTCP46 also interacted with a bric-a-brac/tramtrack/broad (BTB) protein, MdBT2, that is responsive to high light intensity, which ubiquitinated MdTCP46 and mediated its degradation via the 26S proteasome pathway. Our results demonstrate that the dynamic regulatory module MdBT2-MdTCP46-MdMYB1 plays a key role in modulating anthocyanin biosynthesis at different light intensities in apple, and provides new insights into the post-transcriptional regulation of TCP proteins.

Keywords: Anthocyanin accumulation, apple, high-light intensity, *Malus domestica*, post-transcriptional regulation, TCP transcription factor.

Introduction

Anthocyanins are a type of water-soluble pigment that are found in plant flowers, fruits, stems, leaves, and seeds. In recent decades, anthocyanin biosynthesis has been studied extensively due to the important antioxidant properties of these compounds and their effects on the appearance of commercial plant produce. Anthocyanins are synthesized through the phenylpropanoid pathway, in which a series of enzymes play key roles, including dihydroflavonol 4-reductase (DFR), UDP flavonoid glucosyl transferase (UF3GT), chalcone isomerase (CHI), and chalcone synthase (CHS) (Winkel-Shirley, 1999; Hichri *et al.*, 2011). It is well established that anthocyanin biosynthesis is regulated by the WD40-bHLH-MYB complex at the transcription level through the direct mediation of

the expression of its biosynthetic genes (Carbone *et al.*, 2009; Hichri *et al.*, 2011). External stimuli, such as temperature, light, water, nutrients, and exogenous hormones, also play key roles in the regulation of anthocyanin biosynthesis (Winkel-Shirley, 2001, 2002; Carbone *et al.*, 2009; Jaakola, 2013; Honda and Moriya, 2018).

Light is one of the most important environmental factors regulating anthocyanin biosynthesis (Talos *et al.*, 2006; Jaakola, 2013). Numerous studies have demonstrated that light stimulates the accumulation of anthocyanin and that its biosynthesis does not occur in the dark (Meng *et al.*, 2004; Azuma *et al.*, 2012; Zoratti *et al.*, 2014; Guan *et al.*, 2016; Jiang *et al.*, 2016). The light quality also affects biosynthesis, especially ultraviolet

and blue light (Ordidge *et al.*, 2012; Henry-Kirk *et al.*, 2018; Tao *et al.*, 2018; Zhang *et al.*, 2018a). Studies on apple, strawberry, pear, and peach have shown that ultraviolet and blue light treatments promote the expression of transcription factors (TFs) such as MYB, BBX, ERF, and HY5, which in turn activate the expression of anthocyanin biosynthetic genes and ultimately lead to increased anthocyanin levels (Ubi *et al.*, 2006; Gong *et al.*, 2015; Henry-Kirk *et al.*, 2018; Zhang *et al.*, 2018a; An *et al.*, 2019a; Fang *et al.*, 2019; Ni *et al.*, 2019). Light intensity also affects anthocyanin biosynthesis (Jaakola, 2013; Trojak and Skowron, 2017; Zhang *et al.*, 2018b). Previous studies have suggested that TCP and MYB TFs may play roles in anthocyanin accumulation and may be mediated by conditions of different light intensity (Talos *et al.*, 2006; Viola *et al.*, 2016).

In many species, MYB1 and its orthologs (MYB10 and MYBA) play key roles in the regulation of anthocyanin biosynthesis, and they are known to be positive regulators of accumulation that is mediated by various environmental and hormone signaling pathways (Talos *et al.*, 2006; Ban *et al.*, 2007; Espley *et al.*, 2007; Lin-Wang *et al.*, 2010; Niu *et al.*, 2010; Telias *et al.*, 2011; Schwinn *et al.*, 2016; Yi *et al.*, 2018). In apple (*Malus domestica*), overexpression of *MdMYB1* promotes accumulation by activating the transcripts of anthocyanin biosynthetic genes such as *MdDFR* and *MdUF3GT* (Talos *et al.*, 2006; Ban *et al.*, 2007; Espley *et al.*, 2007). Previous studies have demonstrated that *MdMYB1* can coordinate with *MdbHLH3*, *MdERF3*, *MdbZIP44*, *MdWRKY40*, and *MdERF38* to regulate the biosynthesis of anthocyanin that is promoted by low temperature, ethylene, abscisic acid (ABA), wounding, and drought stress, respectively (Xie *et al.*, 2017; An *et al.*, 2018c, 2018d, 2019c, 2020). In addition, *MdMYB1* undergoes ubiquitination and degradation, that is mediated by *MdCOP1* and *MdBT2* in response to multiple hormonal and environmental signals (Li *et al.*, 2012; Wang *et al.*, 2018).

The teosinte branched1/cycloidea/proliferating (TCP) family encodes specific TFs that feature a TCP domain with a bHLH motif (Cubas *et al.*, 1999; Manassero *et al.*, 2013; Nicolas and Cubas, 2016). In Arabidopsis, 24 TCP proteins have been identified and categorized into two classes based on the presence of the TCP motif (Cubas *et al.*, 1999; Martín-Trillo and Cubas, 2010; Manassero *et al.*, 2013). TCP family proteins have also been discovered in other plant genomes, including rice and apple (Yao *et al.*, 2007; Xu *et al.*, 2014). In apple, they are organized into three classes based on differences in their sequences (Xu *et al.*, 2014). As TFs, TCP proteins regulate the expression of target genes by binding to specific promoter sequences [e.g. GGNCCCAC, GGNCC, GCCCR, or G(T/C)GGNCCC; Aggarwal *et al.*, 2010]. TCP proteins have also been documented to function by directly interacting with a variety of proteins, including other TCPs (Danisman *et al.*, 2012), MYB (Li and Zachgo, 2013), NAC (Weir *et al.*, 2004), and bZIP proteins (Mukhopadhyay and Tyagi, 2015).

There is evidence that TCP proteins play broad roles in plant growth and development, including cell proliferation, gametophyte development, seed germination, leaf and flower development, branching, regulation of the circadian clock, and multiple hormone signals (Corley *et al.*, 2005; Tatematsu *et al.*, 2008; Guo *et al.*, 2010; Koyama *et al.*, 2010; Martín-Trillo and

Cubas, 2010; Pruneda-Paz and Kay, 2010; Kieffer *et al.*, 2011; Sarvepalli and Nath, 2011; Braun *et al.*, 2012; Min *et al.*, 2015; Busch *et al.*, 2019). Although the functions and mechanisms of TCP proteins have been studied extensively, there has been limited examination of their roles in the integration of plant development and environmental signals. Recent studies have shown that TCP15 responds to conditions of high light intensity in Arabidopsis (Viola *et al.*, 2016). In rice, OsTCP19 has been found to positively regulate responses to salt and water-deficit stresses synergistically with OsABI4 (Mukhopadhyay and Tyagi, 2015).

Several TCP proteins have been found to regulate the biosynthesis of secondary metabolites. In Arabidopsis, TCP3 promotes flavonoid accumulation by interacting with the MYB proteins that regulate anthocyanin biosynthesis (Li and Zachgo, 2013). TCP15 acts as a negative regulator in biosynthesis of anthocyanins that is modulated by high light (Viola *et al.*, 2016). In *Artemisia annua*, AaTCP14 activates the expression of *DBR2* and *ALDH1*, two key genes of artemisinin biosynthesis (Ma *et al.*, 2018). In *Lycium ruthenicum*, LrTCP4 has been found to play a key role in the synthesis of kukoamine A (Chabel *et al.*, 2019). Although the regulatory mechanisms of TCP proteins that are involved in plant growth and development through the direct transcriptional regulation of target genes or interaction with other proteins have been widely studied, this is not the case for their transcriptional and post-transcriptional regulation mechanisms. There are just a few studies that have shown that TCP proteins may be regulated by miR319 (Schommer *et al.*, 2014; Bresso *et al.*, 2018; Palatnik and Weigel, 2019, Preprint).

In the present study, we found that *MdTCP46* acted as a positive regulator of anthocyanin biosynthesis induced by high light intensity in apple. *MdTCP46* expression was induced and degradation of the protein was delayed after treatment with high light intensity. *MdTCP46* was also found to interact with *MdMYB1*, and this was essential for anthocyanin biosynthesis induced at high light intensity. *MdTCP46* enhanced the binding activity of *MdMYB1* to its target gene promoters. In addition, *MdTCP46* directly interacted with *MdBT2*, which is a negative modulator of anthocyanin biosynthesis. The expression of *MdBT2* was suppressed by high light intensity at both the transcriptional and post-translational levels. *MdBT2* suppressed the role of *MdTCP46* by inducing its ubiquitination, resulting in subsequent degradation via the 26S proteasome pathway. Our findings uncover a potential regulatory mechanism of anthocyanin biosynthesis in apple based on the functioning of the BT2-TCP46-MYB1 protein module under different light intensities.

Materials and methods

Plant material and treatments

Uncolored fruit of apple (*Malus domestica*) 'Red Delicious' at 120 d after full bloom were collected from mature trees in an orchard located in Tai'an (Shandong, China). To examine the effects of different light intensities on anthocyanin accumulation in the peel, the fruit were divided into four groups and stored in incubators at 22 °C under different light conditions. The first group was stored with no light. The other groups were stored with 16/8 h photoperiods at either low light (~80 $\mu\text{mol m}^{-2}$

s^{-1}), moderate light ($\sim 150 \mu\text{mol m}^{-2} s^{-1}$), or high light ($\sim 300 \mu\text{mol m}^{-2} s^{-1}$). The fruit were treated for 3–6 d and images were taken. Fruit treated for 1 d were used for gene expression analysis. The peel was detached by hand using a peeler.

Calli of the variety ‘Orin’ and detached leaves of tissue-cultured seedlings of the variety ‘GL-3’ were used for genetic transformation and for determination of the effects of different light intensities on anthocyanin accumulation. The growing conditions of the calli and apple seedlings were as previously described (An et al., 2018b, 2019b).

Plasmid construction

The ORFs of *MdTCP3*, *MdTCP12*, *MdTCP21*, and *MdTCP46* were fused to pGAD424 to generate *MdTCP3*-pGAD, *MdTCP12*-pGAD, *MdTCP21*-pGAD, and *MdTCP46*-pGAD. *MdMYB1* with the autonomously activated domain deleted was fused to pGBD to generate *MdMYB1 Δ* -pGBD. *MdBT2* and its N- and C-terminal fragments were fused to pGBT9 to generate *MdBT2*-pGBD, *MdBT2*-N-pGBD, and *MdBT2*-C-pGBD. The ORFs of *MdTCP46*, *MdMYB1*, and *MdBT2* were fused to pET32a or pGEX 4T-1 to generate *MdTCP46*-pGEX4T-1, *MdTCP46*-pET32a, *MdMYB1*-pET32a, and *MdBT2*-pGEX4T-1. The ORFs of *MdTCP46*, *MdMYB1*, and *MdBT2* were fused to YFP^N or YFP^C to generate *MdTCP46*-YFP^N, *MdTCP46*-YFP^C, *MdMYB1*-YFP^C, and *MdBT2*-YFP^N.

To generate constructs for the dual luciferase assays, the ORFs of *MdTCP46* and *MdMYB1* were inserted into pGreenII62-SK. The promoter sequences of *MdDFR* and *MdUFGT* were cloned into pGreenII0800-LUC.

The ORF of *MdTCP46* was inserted into IL60-2 and TRV2 to generate *MdTCP46*-IL60-2 and *MdTCP46*-TRV2, respectively. IL60-1 and TRV1 acted as auxiliary plasmids. The *MdTCP46* transient overexpression construct (*MdTCP46*-pIR) consisted of IL60-1 and *MdTCP46*-IL60-2. And the *MdTCP46* transient antisense construct (*MdTCP46*-TRV) consisted of TRV1 and *MdTCP46*-TRV2.

To generate *MdTCP46*-overexpression (-OX) lines, the ORFs of *MdTCP46* were fused to pCXS-N-GFP. To generate *MdBT2*-OX, the ORFs of *MdBT2* were fused to pRI101. To generate *MdTCP46*-antisense (-Anti), *MdMYB1*-Anti, and *MdBT2*-Anti, sequences of *MdTCP46*, *MdMYB1*, and *MdBT2* were inserted into the pCXS-N vector. All primers are listed in Supplementary Table S3 at JXB online.

Genetic transformation

Transgenic apple calli, leaves, and fruit, and Arabidopsis were obtained as previously described (An et al., 2018b, 2019c). In brief, wild-type (WT) apple calli were incubated with *Agrobacterium* carrying recombinant plasmids and genetically transformed calli were screened on selective media (An et al., 2018b, 2019c). Transgenic Arabidopsis seedlings were obtained by the floral dip method (Clough and Bent, 1998). Transient transgenic apple leaves were generated by vacuum infiltration (An et al., 2018b, 2019c).

Apple injection assays

The overexpression viral vector *MdTCP46*-IL60-2 was generated by inserting the CDS of *MdTCP46* into the IL60-2 vector. The IL60-1 vector was used as an auxiliary plasmid. The antisense viral vector *MdTCP46*-TRV2 was obtained by cloning the CDS of *MdTCP46* into the TRV2 vector. The TRV1 vector was used as an auxiliary plasmid. The TRV vectors were introduced into *Agrobacterium tumefaciens* LBA4404. The mixed vectors and the *A. tumefaciens* solutions were injected into the fruit peels.

Measurement of anthocyanin contents

Anthocyanin was extracted using an extraction buffer containing anhydrous ethanol and hydrochloric acid as previously described (An et al., 2018c, 2019c). In brief, samples were placed in the extraction buffer for 5 h. After centrifugation, the supernatant was collected, and its absorption

values at 530, 620, and 650 nm were determined using a spectrophotometer (Soptop, Shanghai, China) (An et al., 2018c, 2019c).

Quantitative real-time PCR

RNA extraction was performed using a RNAsplant plus Reagent (Tiangen) as previously described (An et al., 2018a, 2020). Quantitative real-time PCR (qRT-PCR) was conducted to identify transgenic material and to detect *MdTCP46* and *MdBT2* transcripts. To determine the light responses of *MdTCP46* and *MdBT2*, fruit of ‘Red Delicious’ were sampled at 120 d after full bloom and kept in bags in the dark before being placed in the different light-intensity conditions. Three biological replicates and three technical replicates were used in all qRT-PCR reactions. All primers are listed in Supplementary Table S3.

Yeast two-hybrid assays

The pGAD424 and pGBT9 vectors (Clontech) were used to perform yeast two-hybrid (Y2H) assays. The pGAD424 vector contained a GAL4 activation domain, and the pGBT9 vector contained a GAL4 binding domain. The ORFs of the *MdTCP46* and *MdMYB1* sequences lacking the autonomously activated fragments were fused to the pGAD424 and pGBT9 vectors, respectively. *MdTCP3*-pGAD, *MdTCP12*-pGAD, *MdTCP21*-pGAD, *MdTCP46*-pGAD, *MdMYB1 Δ* -pGBD, *MdBT2*-pGBD, *MdBT2*-N-pGBD, and *MdBT2*-C-pGBD were constructed as described above. The genetic transformation of Y2H Gold yeast cells (Clontech) was accomplished by PEG induction. Transformed yeast cells were cultured on a selective medium for 3 d, and Y2H assays were performed as previously described (An et al., 2019b, 2020). The pGAD424 and pGBT9 empty vectors were used as negative controls.

Pull-down assays

The pET32a and pGEX4T-1 vectors (Novagen) were used to perform pull-down assays. The pET32a vector contained a HIS tag, and pGEX4T-1 contained a GST tag. *MdTCP46*-pGEX4T-1, *MdTCP46*-pET32a, *MdMYB1*-pET32a, and *MdBT2*-pET32a were constructed as described above. The fusion proteins of *MdTCP46*-GST, *MdTCP46*-HIS, *MdMYB1*-HIS, and *MdBT2*-HIS were obtained by isopropyl β -D-1-thiogalactopyranoside (IPTG) induction. A polyhistidine binding resin pull-down kit (Pierce™ His Protein Interaction Pull-Down Kit, ThermoFisher Scientific) was used in this study. GST proteins were used as negative controls. The eluted solution was treated with HIS and GST antibodies (Abmart, Shanghai, China) and pull-down assays were performed as previously described (An et al., 2019b, 2020).

Bimolecular fluorescence complementation assays

The pSPYNE-35S/pUC-SPYNE and pSPYCE-35S/pUC-SPYCE vectors (Clontech) were used to perform bimolecular fluorescence complementation (BiFC) assays. The pSPYNE-35S/pUC-SPYNE vector contained a YFP^N domain, and the pSPYCE-35S/pUC-SPYCE vector contained a YFP^C domain. *MdTCP46*-YFP^N, *MdTCP46*-YFP^C, *MdMYB1*-YFP^C, and *MdBT2*-YFP^N were constructed as described above. Onion epidermis was incubated with an *Agrobacterium* solution carrying the relevant plasmid and the cells were observed 3 d later using a FV3000 fluorescence microscope (Olympus). BiFC assays were performed as previously described (An et al., 2019b, 2020).

Screening of proteins interacting with *MdMYB1*

An apple gene library and the *MdMYB1 Δ* -pGBD plasmid were prepared to screen *MdMYB1*-interacting proteins using a Y2H system, as previously described (An et al., 2018d). Four potential interacting proteins were obtained, namely *MdTCP3* (accession no. MDP0000243495), *MdTCP12* (MDP0000173048), *MdTCP21* (MDP0000851695), and *MdTCP46* (MDP0000319941). Given the false-positive phenomenon of Y2H screening, the interactions were further confirmed through

one-to-one Y2H assays. Only MdTCP46 was found to be a direct interacting protein with MdMYB1.

Electromobility shift assays

Electromobility shift assays (EMSAs) were conducted to determine the effects of MdTCP46 on the binding activity of MdMYB1 to the promoters of *MdDFR* and *MdUF3GT*. MdTCP46-HIS and MdMYB1-HIS fusion proteins were obtained by IPTG-mediated induction. The probe was labeled with biotin by the Sangon Biotech Co. (Shanghai, China). Designated proteins and probes were mixed in the binding buffer for 25 min. The binding and free probes were separated by acrylamide gel, and EMSAs were performed as previously described (An *et al.*, 2018d).

Dual-luciferase assays

The pGreenII62-SK and pGreenII0800-LUC vectors were used to perform dual-luciferase assays. The pGreenII62-SK vector contained a 35S promoter, and the pGreenII0800-LUC vector contained a LUC tag. *MdTCP46*-pGreenII62-SK, *MdMYB1*-pGreenII62-SK, *proMdDFR*-pGreenII0800-LUC, and *proMdUF3GT*-pGreenII0800-LUC were constructed as described above. The plasmid combinations were injected into the back of a leaf of *Nicotiana benthamiana* by *Agrobacterium*-mediated transformation. The pGreenII62-SK and pGreenII0800-LUC empty vectors were used as negative controls. Fluorescence activity was detected using a fluorescence detection kit (Promega) (An *et al.*, 2018d).

Protein degradation assays in vitro

To determine the effects of different light intensities on the stability of the MdTCP46 and MdBT2 proteins, fruit of 'Red Delicious' (120 d after full bloom) were subjected to the low- and high-light treatments for 3 d. The peels were collected, and total proteins were extracted and incubated with the MdTCP46-GST and MdBT2-HIS fusion proteins. Samples were taken at 0–6 h of incubation and protein residues were determined using HIS and GST antibodies (Abmart).

To determine the effects of MdBT2 on the stability of the MdTCP46 protein, WT and transgenic apple calli extracts were incubated with the MdTCP46-GST protein. Samples were taken at 0–6 h of incubation and protein residues were determined using a GST antibody (Abmart). Protein degradation assays *in vitro* were performed as previously described (An *et al.*, 2019b, 2020). Briefly, calli were ground in liquid nitrogen, soaked with protein extraction liquid, and the supernatant was obtained following centrifugation.

To examine the effects of the MG132 proteasome inhibitor, total proteins from calli were pre-treated with 100 μ M MG132 dissolved in DMSO for 0.5 h. DMSO alone was used as the blank control.

Detection of protein ubiquitination in vivo

Detection of protein ubiquitination *in vivo* was performed using a Pierce™ Co-Immunoprecipitation Kit (ThermoFisher Scientific). In brief, the MdTCP46-GFP protein was extracted from apple calli using a GFP antibody (Abmart) and immunoprecipitated proteins were examined using ubiquitin and GFP antibodies (Abmart). Protein ubiquitination detection *in vivo* was performed as previously described (An *et al.*, 2019c).

Statistical analyses

All experiments were conducted three times with consistent results, and data are presented for one representative experiment. Experimental results were analysed using the DPS v7.05 software by one-way ANOVA and LSD *post hoc* tests.

Accession numbers

Sequence data in this study can be obtained from the apple gene function and gene family (<https://gfdb.sdau.edu.cn>; <https://www.rosaceae.org/node/1>), TAIR (<https://www.arabidopsis.org/>), and NCBI (<https://www.ncbi.nlm.nih.gov/>) databases under the following accession numbers: *MdTCP3* (MDP0000243495), *MdTCP12* (MDP0000173048), *MdTCP46* (MDP0000319941), *MdTCP21* (MDP0000851695), *MdBT2* (MDP0000151000), *MdMYB1* (MDP0000259614), *MdDFR* (MDP0000494976), and *MdUF3GT* (MDP0000405936).

Results

MdMYB1 acts as a positive regulator of anthocyanin accumulation under high light intensity

It has been demonstrated that light promotes anthocyanin accumulation in apple, strawberry, pear, and peach (Ubi *et al.*, 2006; Gong *et al.*, 2015; Henry-Kirk *et al.*, 2018; Zhang *et al.*, 2018b; An *et al.*, 2019a; Fang *et al.*, 2019; Ni *et al.*, 2019). In this study, uncolored 'Red delicious' apple fruit were stored in incubators under different conditions of light intensity. Compared to storage under constant dark conditions, fruit consistently turned red after treatment with light, and higher light intensities clearly up-regulated the expression of genes related to anthocyanin biosynthesis, resulting in higher contents (Supplementary Fig. S1A–C).

MdMYB1 is known to be involved in anthocyanin biosynthesis, and overexpression of *MdMYB1* contributes to its accumulation in apple (Takos *et al.*, 2006; Ban *et al.*, 2007; Espley *et al.*, 2007). We constructed a *MdMYB1*-antisense suppression plasmid and transformed it into apple calli (Supplementary Fig. S2A). In the wild-type (WT) plants, moderate and high light intensities progressively and significantly increased anthocyanin accumulation compared to low-light conditions (Supplementary Fig. S1D, E). In contrast, *MdMYB1*-Anti plants showed no difference between low and moderate light, and only a relatively small increase in accumulation under high-light conditions. These results indicated that MdMYB1 was essential for the induction of anthocyanin biosynthesis under high light intensity.

MdTCP46 interacts with *MdMYB1*

We conducted a search for proteins that interact with MdMYB1 in a yeast screening library. The MdMYB1 protein with the autonomously activated domains removed was fused to pGBT9 to generate MdMYB1^Δ-pGBD. An apple TCP protein was obtained (An *et al.*, 2018b) and a NCBI BLAST search showed it to be a TCP15-like protein (Supplementary Fig. S3). We named it as MdTCP46, according the systematic classification of the apple TCP family (Xu *et al.*, 2014).

The physical interaction between MdTCP46 and MdMYB1 was confirmed by three different assays (Fig. 1). First, *MdTCP46*-pGAD and *MdMYB1* Δ -pGBD were constructed and transformed into Gold yeast cells for Y2H assays. Only yeast cells with both MdTCP46 and MdMYB1 grew normally on selective medium (–T/–L/–H/–A) (Fig. 1A), suggesting a direct interaction. Second, fusion proteins were prepared for pull-down assays and the results indicated that MdTCP46-GST was pulled-down by MdMYB1-HIS (Fig. 1B). Third, BiFC assays were developed that linked *MdTCP46* with the N-terminus of YFP (*MdTCP46*-YFP^N) and *MdMYB1* with the C-terminus of YFP (*MdMYB1*-YFP^C). The resulting

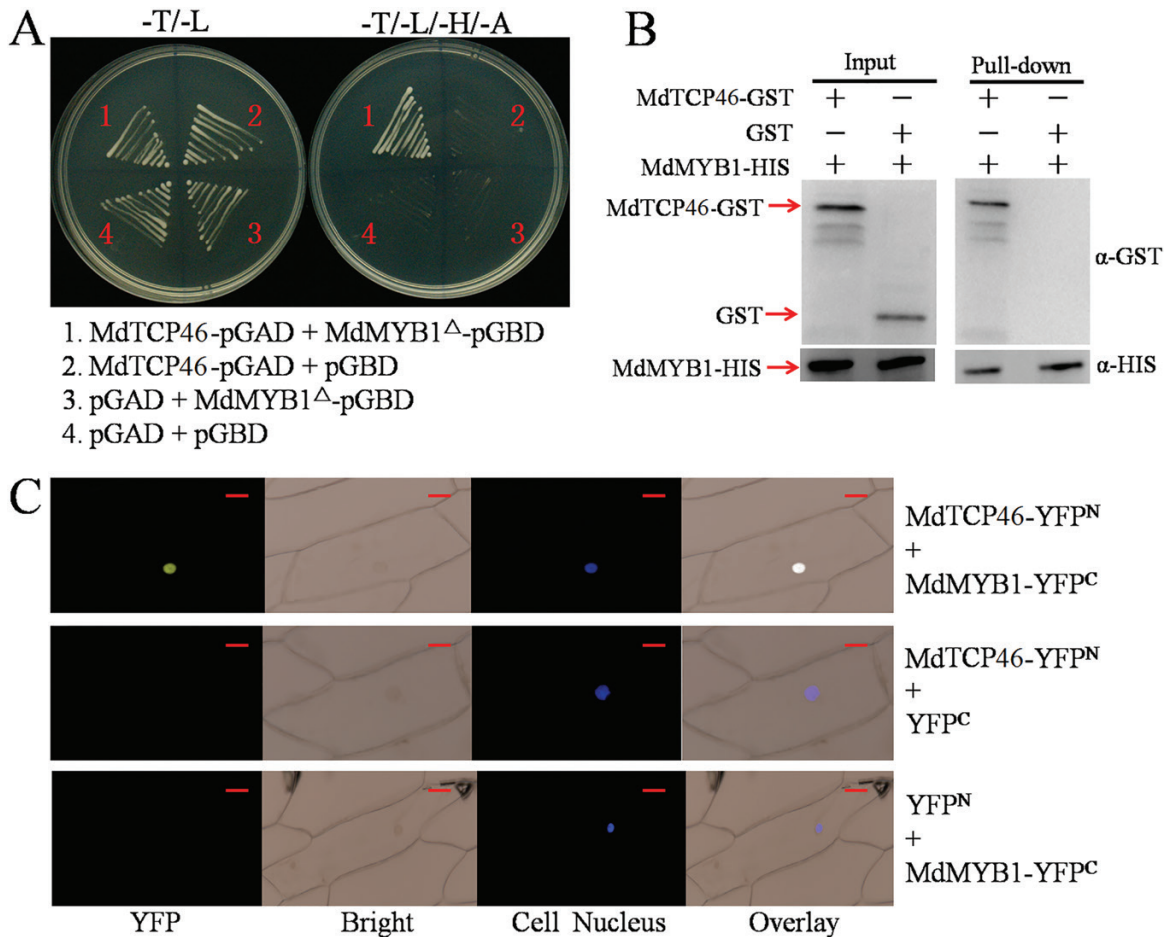


Fig. 1. Apple MdTCP46 interacts with MdMYB1. (A) Yeast two-hybrid assays. The ORFs of the *MdTCP46* and *MdMYB1* sequences lacking the autonomously activated fragments were fused to the pGAD424 and pGBT9 vectors, respectively. The pGAD424 and pGBT9 empty vectors were used as negative controls. -T/-L, SD medium lacking Trp and Leu; -T/-L/-H/-A, SD medium lacking Trp, Leu, His, and Ade. (B) Pull-down assays. The ORFs of *MdMYB1* and *MdTCP46* were fused to the pET32a and pGEX4T-1 vectors, respectively. The MdMYB1-HIS and MdTCP46-GST fusion proteins were obtained from *E. coli* expression. GST proteins were used as negative controls. The eluted solution was probed using HIS and GST antibodies. (C) Bimolecular fluorescence complementation assays. The ORFs of *MdTCP46* and *MdMYB1* were fused to the YFP^N and YFP^C vectors, respectively. Fluorescence was examined using a confocal laser-scanning microscope. Scale bars are 10 μm. (This figure is available in colour at JXB online.)

fluorescence signals showed that MdTCP46 interacted with MdMYB1 in the nucleus (Fig. 1C). Collectively, these data indicated that MdTCP46 physically interacts with MdMYB1.

MdTCP46 promotes anthocyanin biosynthesis

MdTCP46 is a TCP family protein and was found to contain a conserved bHLH domain at the N terminus (Fig. 2A). Compared to TCP proteins from different or species organisms, it exhibited the highest homology with the *Pyrus bretschneideri* protein, PbTCP.

When apple fruit were stored under different light intensities, qRT-PCR analysis indicated that moderate and high light significantly induced the expression of *MdTCP46* (Fig. 2B). The abundance of the MdTCP46 protein was also examined. MdTCP46-GST, an *E. coli* fusion protein, was probed with GST antibodies under either low or high light treatment. The results indicated that high light delayed MdTCP46 protein degradation (Fig. 2C). Furthermore, inclusion of the MG132 proteasome inhibitor blocked degradation completely, indicating that MdTCP46 is degraded by the 26S-proteasome

machinery. These results suggested that *MdTCP46* was responsive to high light intensity at both the transcriptional and post-translational levels.

To assess the biological role of MdTCP46 in the regulation of anthocyanin biosynthesis, transgenic apple fruit and *Arabidopsis* were generated (Supplementary Fig. S2B). The MdTCP46-pIR construct was used to generate *MdTCP46*-overexpression (-OX) lines and the MdTCP46-TRV construct was used to generate *MdTCP46*-antisense (-Anti) lines. Compared to the WT controls, overexpression of *MdTCP46* in both apple fruit and *Arabidopsis* seedlings clearly increased anthocyanin accumulation whilst antisense suppression decreased it (Fig. 2D-I). These results indicate an essential and positive role of *MdTCP46* in anthocyanin accumulation.

MdTCP46 is essential for anthocyanin biosynthesis mediated by high light intensity

We generated stable transgenic apple calli and transient transgenic leaves with either overexpression of *MdTCP46* (*MdTCP46*-OX) or with antisense suppression of *MdTCP46*

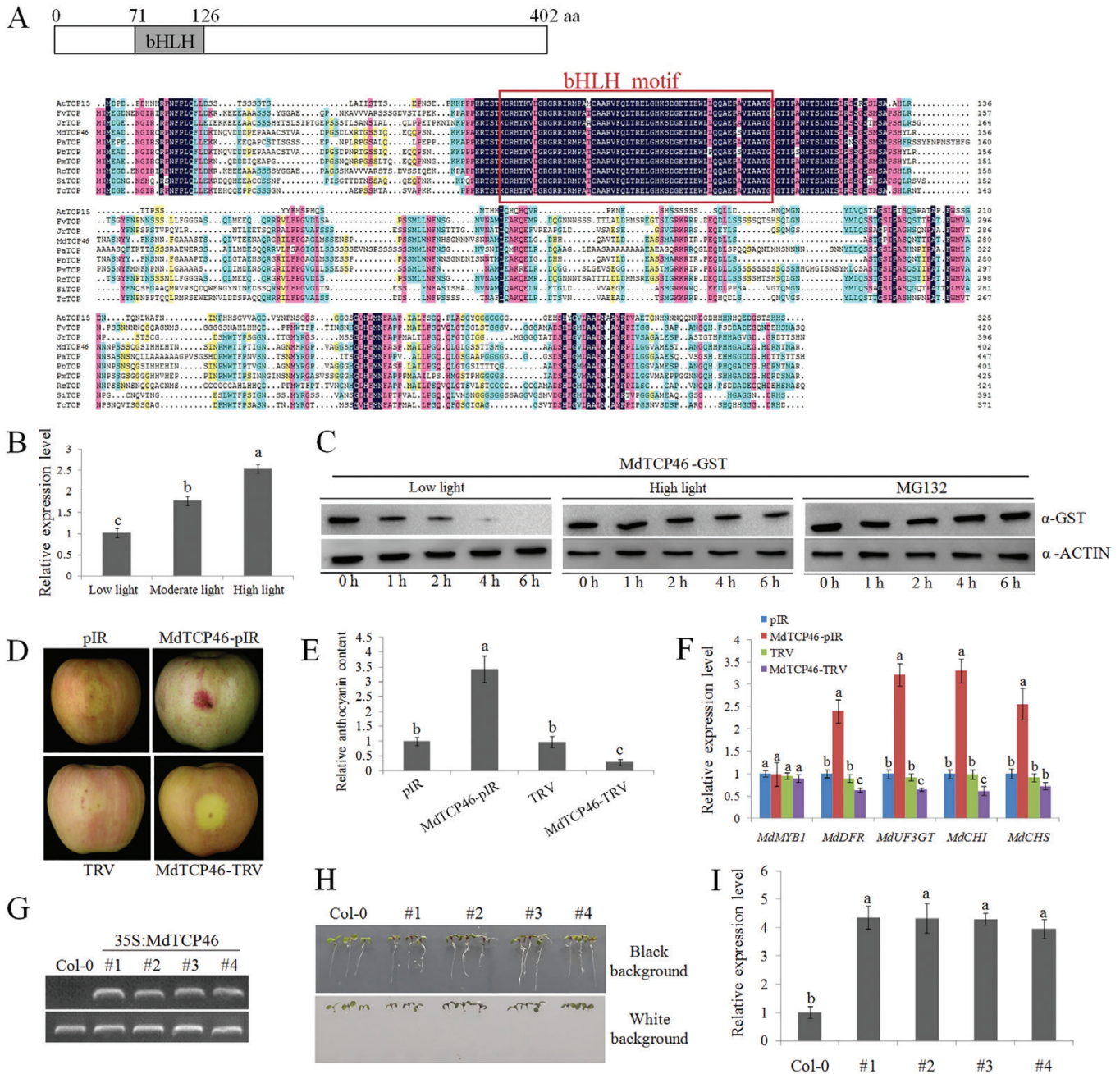


Fig. 2. Overexpression of *MdTCP46* promotes anthocyanin biosynthesis in apple. (A) Multiple alignment of the bHLH domain in 10 TCP proteins obtained from the NCBI database. PbTCP, *Pyrus × bretschneideri* (XP_009360352.1); PmTCP, *Prunus mume* (XP_008221641.1); RcTCP, *Rosa chinensis* (XP_024194958.1); FvTCP, *Fragaria vesca* (XP_004297311.1); PaTCP, *Parasponia andersonii* (PON70380.1); JrTCP, *Juglans regia* (XP_018817718.1); MtTCP, *Malus domestica* (MDP000031994.1); AtTCP15, *Arabidopsis thaliana* (AT1G69690.1). The bHLH motif is indicated. (B) Transcription of *MdTCP46* under different light intensities using qRT-PCR. Plants were treated for 3 d and expression was normalized to the *actin* gene. Values are relative to the low-light treatment, which was set as 1. (C) Detection of the *MdTCP46*-GST fusion protein after dark and moderate light treatments. ‘Red Delicious’ apple fruit were treated with low or high light for 3 d. Total proteins were extracted from the peels and were incubated with purified *MdTCP46*-GST protein for 0–6 h. For treatment with the proteasome inhibitor MG132, total proteins of fruit subjected to low light were pre-treated with 100 μ M MG132 for 0.5 h before the sampling began. ACTIN was used as an internal reference. (D) Apple peel injection assays. Uncolored ‘Red Delicious’ fruit were injected with mixed vectors or *A. tumefaciens* solutions and stored in a phytotron under the high-light treatment for 3 d. pIR, IL60-1+IL60-2; *MdTCP46*-pIR, IL60-1+*MdTCP46*-IL60-2; TRV, TRV1+ TRV2; *MdTCP46*-TRV, TRV1+*MdTCP46*-TRV2. pIR are overexpressors (OX); TRV are antisense suppressors (Anti). (E) Anthocyanin contents of the fruit peels shown in (D). Contents are expressed relative to pIR, the value of which was set as 1. (F) Expression of genes related to anthocyanin biosynthesis in the fruit peels shown in (D) as determined by qRT-PCR. Expression was normalized to the *actin* gene. Values are expressed relative to pIR, which were set as 1. (G) qRT-PCR detection of *MdTCP46* expression levels in Arabidopsis Col-0 seedlings and in overexpressing transgenic lines. The lower panels show the *ACTIN* gene, which was used as the internal control. (H) Phenotypes of Arabidopsis Col-0 and *MdTCP46*-overexpressing lines and (I) relative expression of *MdTCP46*. Expression was normalized to the *ACTIN* gene. Values are expressed relative to Col-0, which was set as 1. All experiments were performed three times with similar results, and representative data from one experiment are shown. Data are means (\pm SD), $n=6$. Different letters indicate significant differences as determined by one-way ANOVA and LSD tests ($P<0.05$). (This figure is available in colour at JXB online.)

(*MdTCP46*-Anti) (Supplementary Fig. S2C, D). Compared to the WT controls, overexpression of *MdTCP46* promoted anthocyanin accumulation in both the calli and leaves, whilst antisense suppression of *MdTCP46* reduced it (Fig. 3). The expression of five genes related to anthocyanin biosynthesis were examined in the calli, namely *MdMYB1*, *MdDFR*, *MdUF3GT*, *MdCHI*, and *MdCHS*. All five were expressed at higher levels when *MdTCP46* was overexpressed (Fig. 3C). The effect of *MdTCP46* expression on anthocyanin accumulation was more obvious as light intensity increased (Fig. 3A, B, D, E), indicating

that it was essential for accumulation mediated by high light intensity.

MdTCP46 promotes anthocyanin biosynthesis when *MdMYB1* is suppressed

Since both *MdTCP46* and *MdMYB1* play positive roles in anthocyanin biosynthesis induced by high light intensity in apple, we examined the functional relationship between them. Transgenic apple calli were generated to overexpress *MdTCP46*

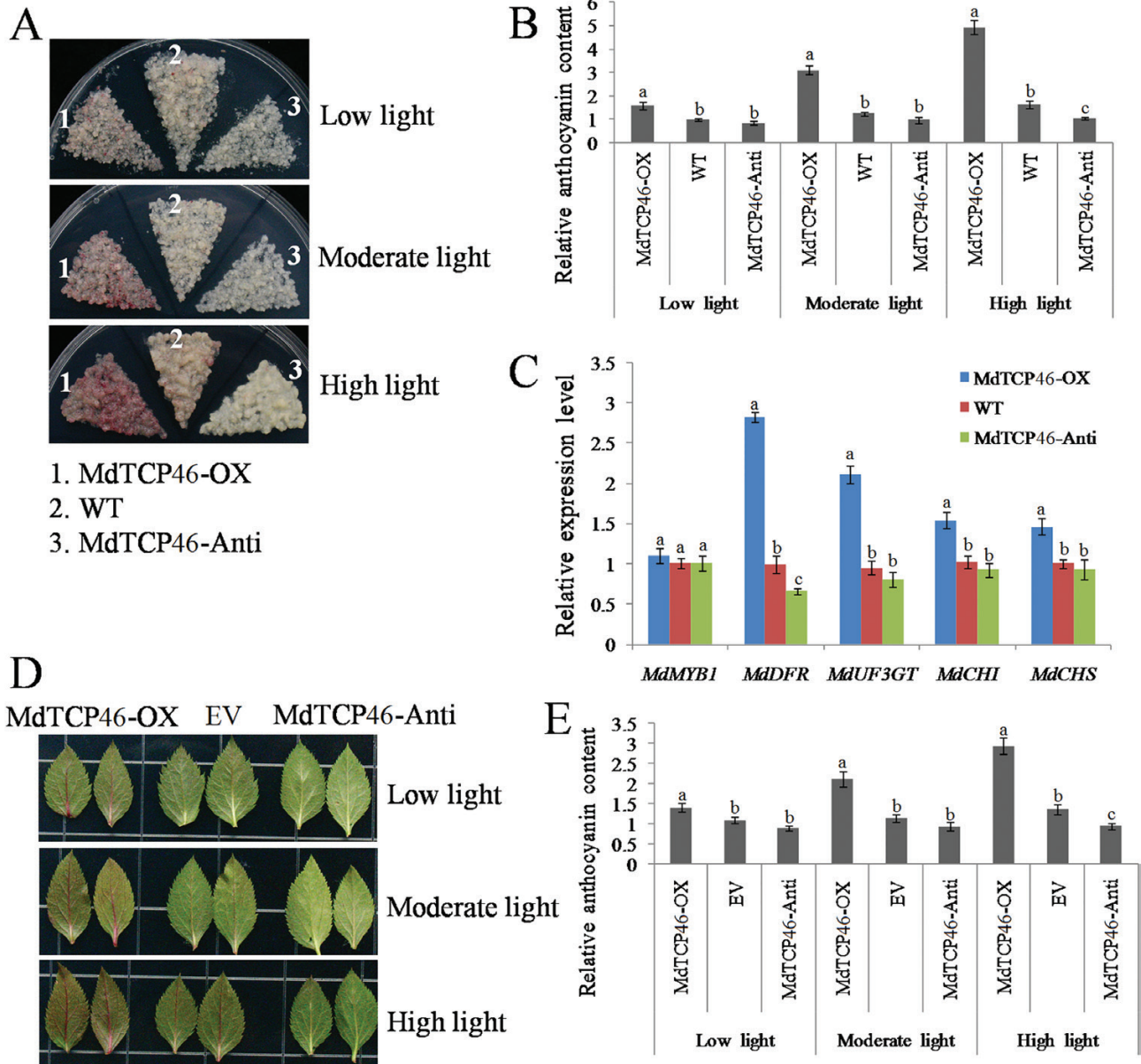


Fig. 3. *MdTCP46* promotes light-induced anthocyanin biosynthesis in apple. Transgenic apple calli (15 d old) and leaves of *MdTCP46*-overexpressing (-OX) and *MdTCP46*-antisense (-Anti) were subjected to different light intensities for 5 d. (A) Phenotypes of calli of the transgenic lines and the wild-type (WT) and (B) their anthocyanin contents. The content of low light-treated WT was used as a reference and set to 1. (C) The expression of genes related to anthocyanin biosynthesis in apple calli as determined by qRT-PCR. The expression of the WT was used as a reference and set to 1. (D) Phenotypes of transient transgenic leaves the empty-vector control (EV) and (E) their anthocyanin contents. The content of low light-treated EV was used as a reference and set to 1. All experiments were performed three times with similar results, and representative data from one experiment are shown. Data are means (\pm SD), $n=4$. Different letters indicate significant differences as determined by one-way ANOVA and LSD tests ($P<0.05$). (This figure is available in colour at JXB online.)

in a *MdMYB1*-suppression background (i.e. *MdTCP46-OX/MdMYB1-Anti*) (Supplementary Fig. S2A). Control samples expressing the *MdTCP46-OX* or *MdMYB1-Anti* constructs individually showed increased and decreased anthocyanin accumulation, respectively (Fig. 4A, B), whilst samples expressing both the constructs showed increased accumulation, but to a lesser extent than observed in *MdTCP46-OX*. These results indicated that *MdTCP46* promoted anthocyanin biosynthesis when *MdMYB1* was suppressed.

MdTCP46 enhances the binding activity of MdMYB1 to its target gene promoters

To determine the functions of *MdTCP46* and *MdMYB1* during anthocyanin biosynthesis, we examined their roles in binding to the promoter sequences of target genes. First, EMSAs were developed using the *MdTCP46-HIS* and *MdMYB1-HIS* fusion proteins and the biotin-labeled probes of *MdDFR* and *MdUF3GT* (Fig. 4C, D; Supplementary Tables S1, S2). Mutated forms of the *MdDFR-Mut* and *MdUF3GT-Mut* probes were used as negative controls. The results showed that *MdMYB1-HIS* alone was able to bind to the *MdDFR*-Probe and *MdUF3GT*-Probe, which was consistent with previous studies (Takos *et al.*, 2006; Ban *et al.*, 2007; Espley *et al.*, 2007). However, the binding became stronger in the presence of *MdTCP46-HIS* fusion proteins (Fig. 4C, D), indicating that *MdTCP46* could improve the binding activity of *MdMYB1* to the *MdDFR* and *MdUF3GT* promoters.

Dual-luciferase assays were also conducted to support the EMSA observations. *MdTCP46* and *MdMYB1* were expressed separately under the control of 35S promoters on the pGreenII 62-SK plasmid vector as effectors, and *LUC* was used as a reporter behind the *MdDFR* or *MdUF3GT* promoter in the pGreenII 0800-LUC plasmid vector (Fig. 4E). It was clear that *MdMYB1* alone was able to drive the expression of the luciferase gene, while *MdTCP46* could not (Fig. 4E, G). *LUC* expression was increased significantly when the constructs expressing both proteins were present, suggesting that *MdTCP46* enhanced the binding activity of *MdMYB1* to the *MdDFR* and *MdUF3GT* promoters.

MdBT2 physically interacts with MdTCP46

We next attempted to identify the potential protein interacting partners of *MdTCP46*. The bric-a-brac/tramtrack/broad (BTB) family protein *MdBT2* has been identified and widely investigated as a repressor of anthocyanin accumulation (An *et al.*, 2018a, 2018d, 2019a, 2019c, 2020; Wang *et al.*, 2018). We therefore conducted three assays to verify the physical interaction between the *MdTCP46* and *MdBT2* proteins. First, *MdTCP46* was cloned into the pGAD424 vector. *MdBT2*, its N-terminus (*MdBT2-N*), and C-terminus (*MdBT2-C*) were individually cloned into the pGBT9 vector (Fig. 5A). The results of Y2H assays revealed that only yeast cells co-transformed with both the full-lengths of *MdTCP46* and *MdBT2* survived on selective medium (Fig. 5A), indicating a direct interaction between *MdTCP46* and *MdBT2* in the cells. Second, pull-down assays were performed that utilized the *E. coli*

expression of *MdBT2-HIS* and *MdTCP46-GST* fusion proteins (Fig. 5B). The polyhistidine binding resin pulled-down the *MdBT2-HIS* and *MdTCP46-GST* fusion proteins, but not when the GST tag was present alone (Fig. 5B). Thus, heterologously expressed *MdTCP46* and *MdBT2* proteins could interact *in vitro*. Third, BiFC assays were performed using onion epidermal cells, and the expression system was transformed with *MdTCP46* linked to the C-terminus of YFP (*MdTCP46-YFP^C*), *MdBT2* linked to the N-terminus of YFP (*MdBT2-YFP^N*), or both. The results showed that *MdTCP46-YFP^C* interacted with *MdBT2-YFP^N* in the nucleus (Fig. 5C). Collectively, these results suggested that *MdTCP46* interacts with *MdBT2* directly *in vivo* and *in vitro*.

MdBT2 is a negative regulator in anthocyanin biosynthesis induced by high light

MdBT2 has previously been identified to repress anthocyanin biosynthesis (An *et al.*, 2018a; Wang *et al.*, 2018). Here, we specifically examined the involvement of *MdBT2* in anthocyanin biosynthesis mediated by different light intensities in apple. *MdBT2-OX* and *MdBT2-Anti* calli were generated (Supplementary Fig. S2E). The overexpression of *MdBT2* reduced the accumulation of anthocyanin under high light, while suppression of *MdBT2* increased anthocyanin levels under all the treatments but particularly under high light (Fig. 6A, B). These results confirmed that *MdBT2* functions as a negative regulator of anthocyanin biosynthesis in apple and is especially important under high light conditions. Interestingly, the expression of *MdBT2* seemed to be regulated by the different light intensities, and it was noticeably downregulated under the high intensity treatment (Fig. 6C). *In vitro* protein degradation assays using *E. coli* expressed *MdBT2-HIS* fusion proteins indicated that the high-light treatment accelerated the degradation of the *MdBT2* protein (Fig. 6D), and this appeared to be mediated by 26S proteasome as the presence of the MG132 proteasome inhibitor completely abolished the degradation of the *MdBT2-HIS* fusion protein. Thus, high light clearly suppressed the expression of *MdBT2* at both the transcriptional and post-translational levels.

MdBT2 suppresses the role of MdTCP46 in anthocyanin biosynthesis induced by high light by inducing its degradation

Given that *MdTCP46* played a positive role and its interacting partner *MdBT2* played a negative role in anthocyanin accumulation induced by high light (Figs 3, 6A, B), we examined the physiological relationship between these two genes. *MdTCP46-OX* was co-expressed with *MdBT2-OX* or *MdBT2-Anti* in apple calli and leaves under high light (Supplementary Fig. S2F–H). Compared with the control, all the transgenic plants showed significant increases in anthocyanin content in both calli and leaves (Fig. 7). The greatest increases were observed when expression of *MdBT2* was suppressed, whilst overexpression of *MdBT2* and *MdTCP46* together resulted in anthocyanin levels that were lower than when *MdTCP46* was overexpressed alone (Fig. 7B, D). These

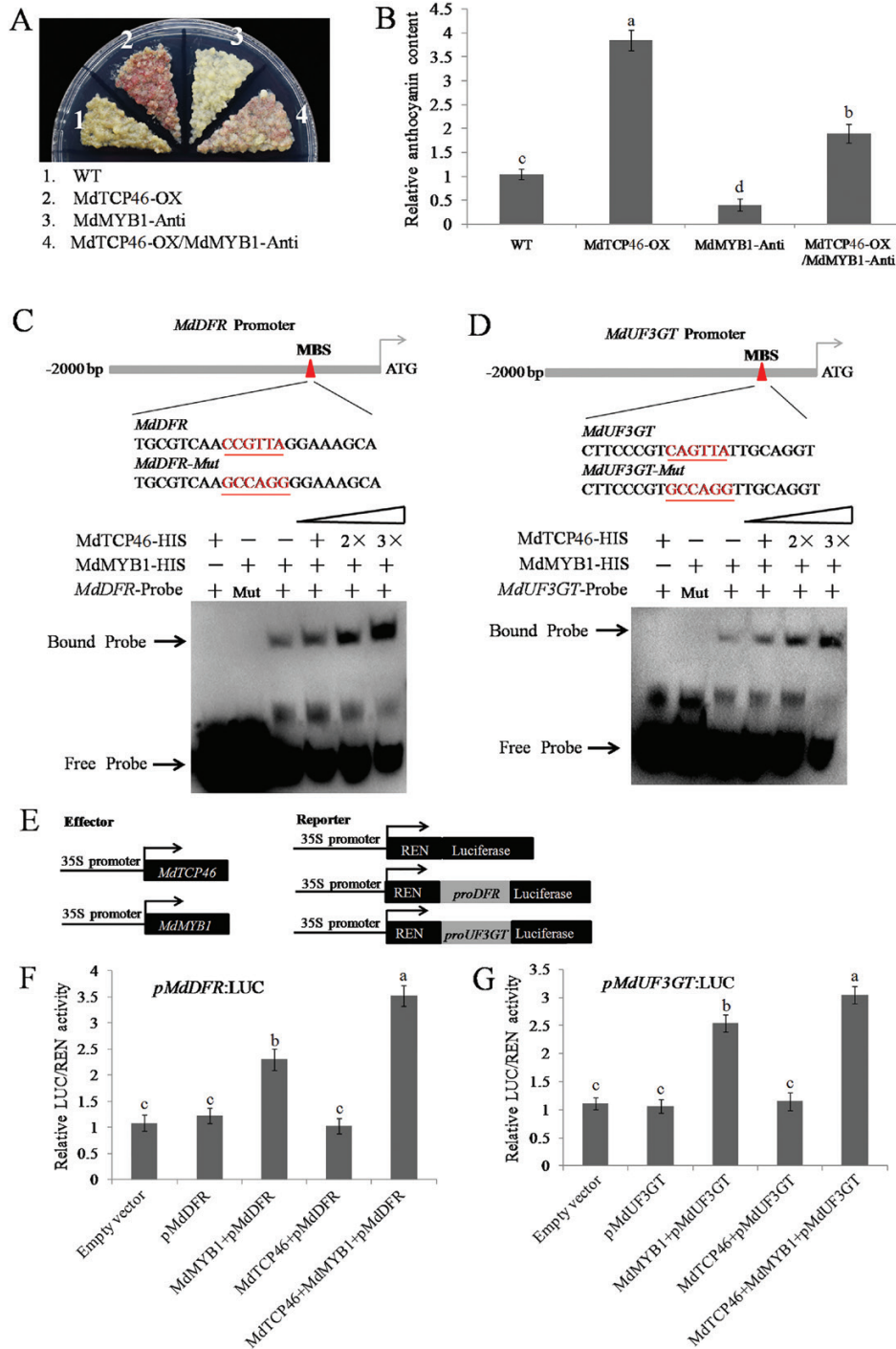


Fig. 4. MdTCP46 enhances the transcriptional activity of MdMYB1 on *MdDFR* and *MdUF3GT*. (A, B) Apple calli (15 d old) of the wild-type (WT), *MdTCP46*-overexpression (-OX), *MdMYB1*-antisense (-Anti), and *MdTCP46*-OX/*MdMYB1*-Anti (overexpression of *MdTCP46* in the background of *MdMYB1*-Anti) were subjected to high light for 5 d. (A) Phenotypes and (B) anthocyanin levels. The content of the WT was used as a reference and set to 1. (C, D) Electromobility shift assays using *MdDFR* and *MdUF3GT* promoter probes. The MBS sequences for MdMYB1 binding and their equivalent mutant forms (-Mut) are underlined. + indicates the presence of corresponding proteins or probes, and - indicates the absence of corresponding of proteins. 2x and 3x indicate increased protein contents. (E) Schematic representation of the LUC reporter vector containing the *MdDFR* and *MdUF3GT* promoters and effector vectors expressing *MdTCP46* or *MdMYB1* under the control of the 35S promoters. The ORFs of *MdTCP46* and *MdMYB1* were fused to the pGreenII 62-SK vector. The promoter sequences of *MdDFR* and *MdUF3GT* were cloned into the pGreenII 0800-LUC vector. (F, G) LUC/REN activities detected by the reporter systems described in (E), which tested the effects of MdMYB1, MdTCP46, and MdMYB1+MdTCP46 on the expression of (F) *MdDFR* and (G) *MdUF3GT*. Empty vector, pGreenII 62-SK + pGreenII 0800-LUC; pMdDFR, pGreenII 62-SK + *proMdDFR*-pGreenII 0800-LUC; pMdUF3GT, pGreenII 62-SK + *proMdUF3GT*-pGreenII 0800-LUC; MdMYB1+pMdDFR, MdMYB1-pGreenII 62-SK + *proMdDFR*-pGreenII 0800-LUC; MdMYB1+pMdUF3GT, MdMYB1-pGreenII 62-SK + *proMdUF3GT*-pGreenII 0800-LUC; MdTCP46+pMdDFR, MdTCP46-pGreenII 62-SK + *proMdDFR*-pGreenII 0800-LUC; MdTCP46+pMdUF3GT, MdTCP46-pGreenII 62-SK + *proMdUF3GT*-pGreenII 0800-LUC; MdTCP46+MdMYB1+pMdDFR, MdTCP46-pGreenII 62-SK + MdMYB1-pGreenII 62-SK + *proMdDFR*-pGreenII 0800-LUC; MdTCP46+MdMYB1+pMdUF3GT, MdTCP46-pGreenII 62-SK + MdMYB1-pGreenII 62-SK + *proMdUF3GT*-pGreenII 0800-LUC. LUC/REN activities of the empty vector were used as references and set to 1. All experiments were performed three times with similar results, and representative data from one experiment are shown. Data are means (±SD), n=3. Different letters indicate significant differences as determined by one-way ANOVA and LSD tests (P<0.05). (This figure is available in colour at JXB online.)

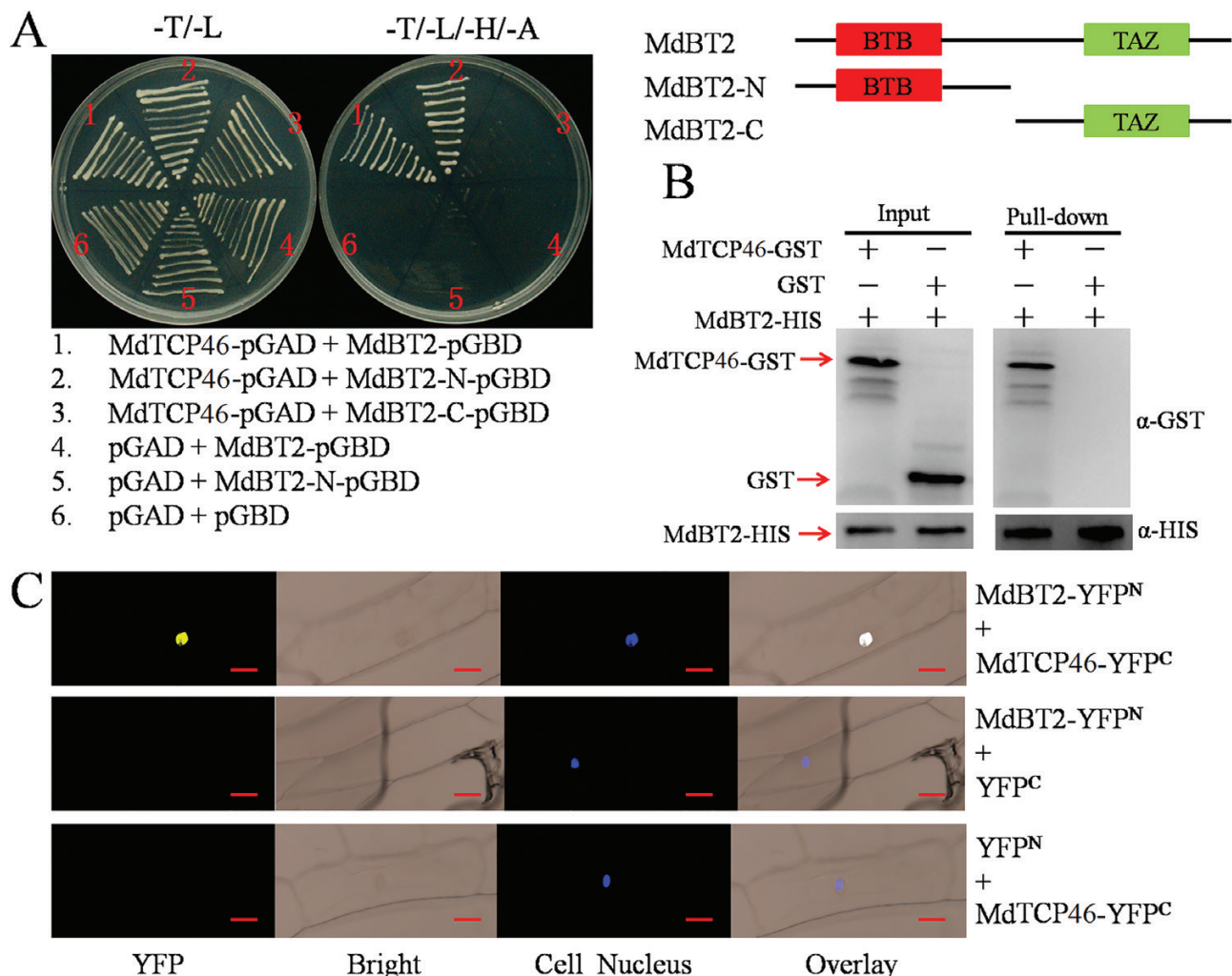


Fig. 5. MdBt2 interacts with MdTCP46. (A) Yeast two-hybrid assays. The ORF of *MdTCP46* and the indicated regions of *MdBt2* (i.e. *MdBt2*, *MdBt2* N terminal, and *MdBt2* C terminal; see schematic diagram to right) were fused to the pGAD and pGBD vectors. The pGAD and pGBD empty vectors were used as negative controls. -T/-L, SD medium lacking Trp and Leu; -T/-L/-H/-A, SD medium lacking Trp, Leu, His, and Ade. (B) Pull-down assays. The ORFs of *MdBt2* and *MdTCP46* were fused to the pET32a and pGEX4T-1 vectors, respectively. The MdBt2-HIS and MdTCP46-GST fusion proteins were obtained from *E. coli* expressions. GST proteins were used as negative controls. The eluted solution was probed with HIS and GST antibodies. (C) Bimolecular fluorescence complementation assays. The ORFs of *MdBt2* and *MdTCP46* were fused to the YFP^N and YFP^C vectors, respectively. Fluorescence was examined using a confocal laser-scanning microscope. Scale bars are 10 μ m. (This figure is available in colour at JXB online.)

results suggested that *MdTCP46* plays a positive role whilst *MdBt2* plays a negative role in anthocyanin accumulation under high-light conditions. In addition, *MdBt2* suppressed the positive role played by *MdTCP46*.

To further explore the interaction mechanism between MdTCP46 and MdBt2, *in vitro* protein degradation assays were conducted. The MdTCP46-GST fusion protein was incubated with total protein extracts from *MdBt2*-OX and *MdBt2*-Anti calli. Consistent with the patterns of anthocyanin accumulation (Fig. 7A, B), degradation of the MdTCP46-GST fusion protein was facilitated by *MdBt2* overexpression, but delayed by *MdBt2* suppression (Fig. 8A). This effect was abolished by the presence of MG132, indicating that the protein degradation was through the 26S proteasome pathway. Indeed, when the MdTCP46-GFP fusion protein was incubated with protein extracts from *MdBt2*-OX calli, strong ubiquitination patterns were observed using Ubi and GFP antibodies with various forms

of ubiquitinated MdTCP46-GFP proteins being detected (Fig. 8B), indicating that a considerable amount of the fusion proteins had been partially degraded and lost the GFP tag. This was consistent with the fact that MdBt2 suppressed the function of MdTCP46 by facilitating its degradation through the 26S proteasome pathway.

MdTCP46 specifically interacts with the MdMYB1 and MdBt2 proteins

There are several TCP family proteins, some of which may have similar or opposing regulatory functions in the same signaling pathways (Li and Zachgo, 2013; Viola *et al.*, 2016). When we screened the MdMYB1-interacting proteins, MdTCP3, MdTCP12, and MdTCP21 were screened out (Xu *et al.*, 2014). Therefore, we cloned these three TCP proteins. In contrast to MdTCP46, none of them exhibited direct interactions with MdMYB1 and MdBt2 in the Y2H assays (Supplementary Fig.

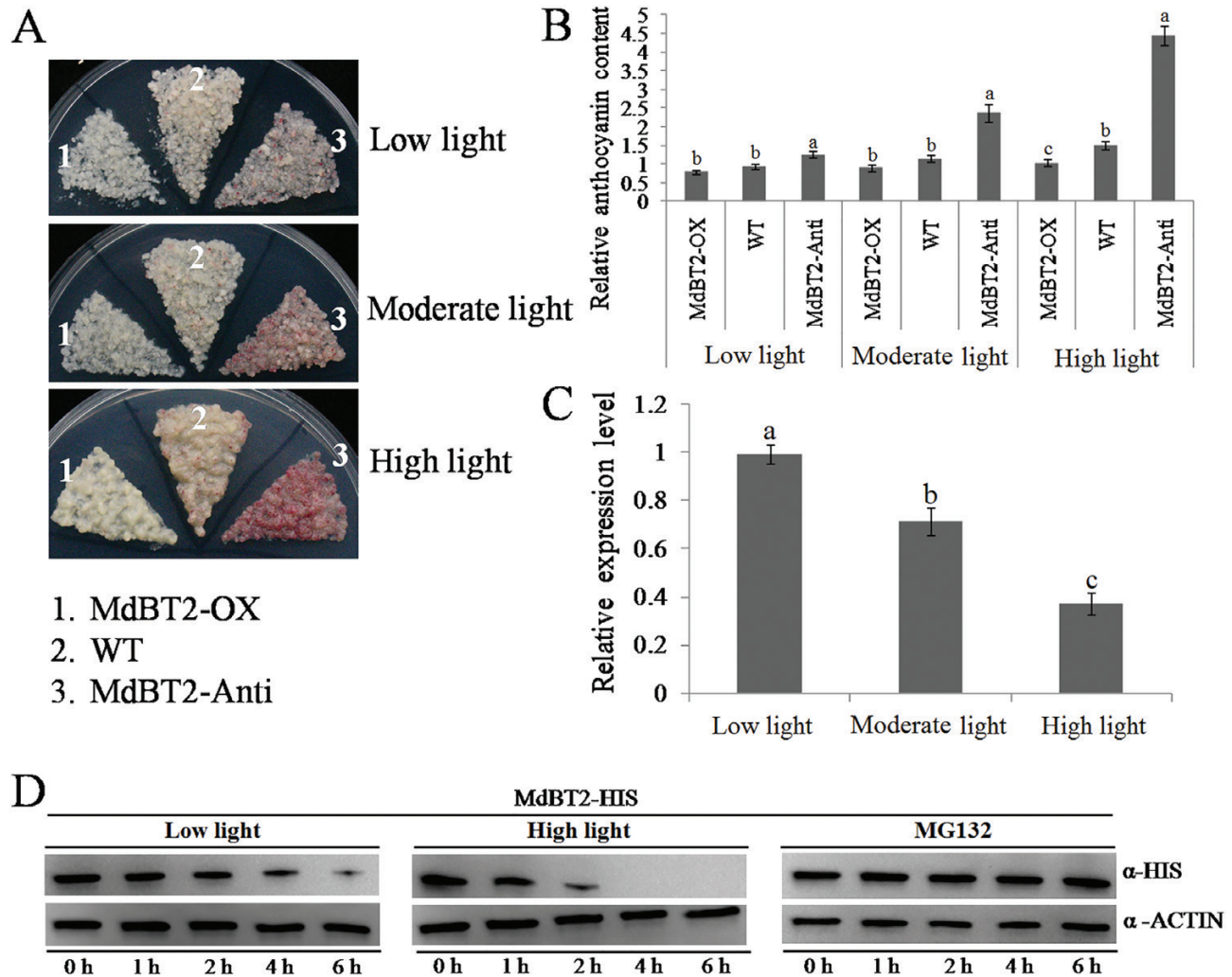


Fig. 6. MdBT2 negatively regulates light-induced anthocyanin biosynthesis. Apple calli (15 d old) of the wild-type (WT) and transgenic *MdBT2*-overexpressing (-OX) and *MdBT2*-antisense (-Anti) lines were subjected to different light intensities for 5 d. (A) Phenotypes and (B) anthocyanin levels. The anthocyanin content the WT under the low-light treatment was used as a reference and set to 1. (C) Expression of *MdBT2* in response to the different light intensities as determined using qRT-PCR. Expression was normalized to the *ACTIN* gene. Values are expressed relative to the low-light treatment, which was set to 1. (D) Detection of the MdBT2-HIS fusion protein after low- and high-light treatments. ‘Red Delicious’ fruit were subjected to the light treatments for 3 d. The total proteins extracted from the peels were incubated with purified MdBT2-HIS protein for 0–6 h. For the treatment with the proteasome inhibitor MG132, the total proteins fruit subjected to low light were pre-treated with 100 μ M MG132 for 0.5 h before the sampling began. ACTIN was used as an internal reference. All experiments were performed three times with similar results, and representative data from one experiment are shown. Data are means (\pm SD), $n=3$. Different letters indicate significant differences as determined by one-way ANOVA and LSD tests ($P<0.05$). (This figure is available in colour at *JXB* online.)

S4). Hence, MdTCP46 seems to specifically interact with the MdMYB1 and MdBT2 proteins.

Discussion

Anthocyanin biosynthesis is regulated by various environmental stimuli (Winkel-Shirley, 2001, 2002; Carbone et al., 2009; Jaakola, 2013; Honda and Moriya, 2018), and light, especially at high intensity, has been implicated in promoting biosynthesis in many species including apple (Jaakola, 2013; Trojak and Skowron, 2017; Zhang et al., 2018b). A positive correlation exists between anthocyanin accumulation and light intensity (Jaakola, 2013; Trojak and Skowron, 2017; Zhang et al., 2018b). Although many proteins have been shown to

participate synergistically in light-modulated anthocyanin accumulation, including MYB, BBX, ERF, and HY5 (Ubi et al., 2006; Gong et al., 2015; Henry-Kirk et al., 2018; Zhang et al., 2018a; An et al., 2019a; Fang et al., 2019; Ni et al., 2019), the underlying molecular mechanisms are not fully understood. Here, we found that MdTCP46 and MdMYB1 play positive roles in anthocyanin biosynthesis induced by high light. In addition, the BTB-domain protein MdBT2 acted as a repressor of anthocyanin biosynthesis under different light intensities by regulating the stability of the MdTCP46 protein.

MdMYB1 is known to be responsive to light treatment in apple (Tacos et al., 2006; Ban et al., 2007; Espley et al., 2007). The importance of MdMYB1 in light-induced anthocyanin biosynthesis has been well established, and it functions by directly activating the expression of genes related to biosynthesis,

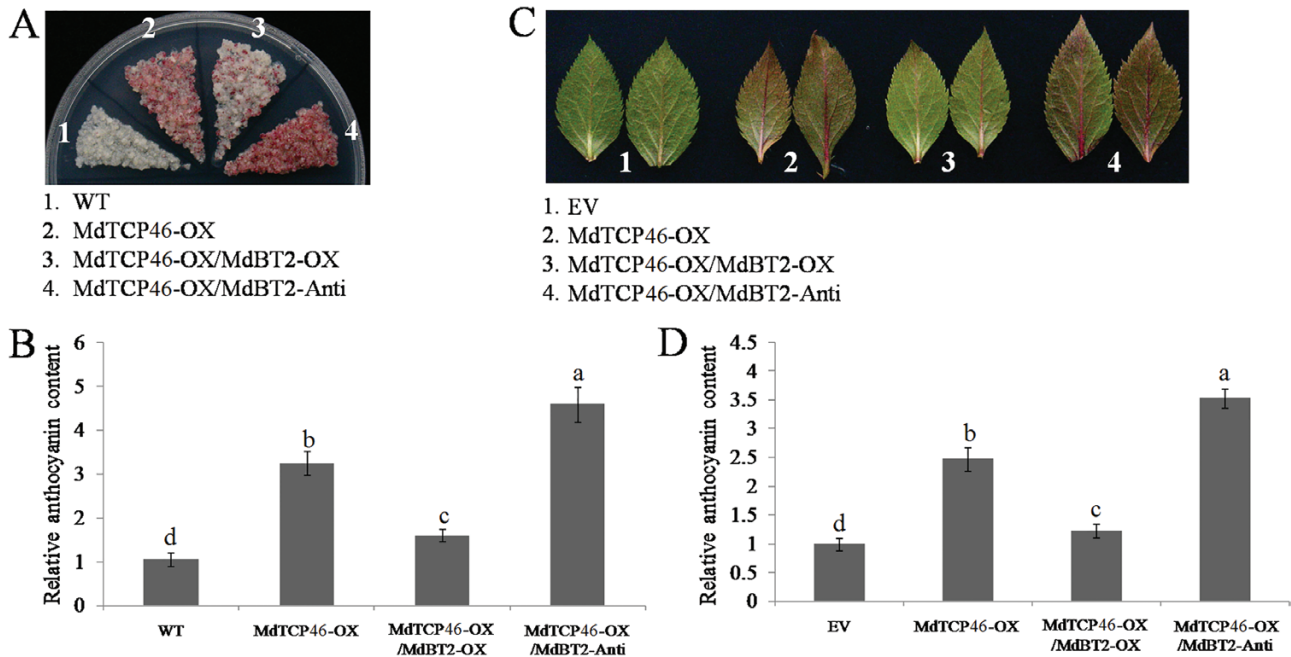


Fig. 7. MdBT2 negatively regulates MdTCP46-promoted anthocyanin biosynthesis. Transgenic apple calli (15 d old) and leaves of *MdTCP46*-overexpressing (-OX), *MdTCP46*-OX/*MdBT2*-OX (overexpression of *MdBT2* in the background of *MdTCP46*-overexpression), and *MdTCP46*-OX/*MdBT2*-Anti (antisense suppression of *MdBT2* in the background of *MdTCP46*-overexpression) were subjected to high light intensity for 5 d. (A) Phenotypes of calli of the transgenic lines and the wild-type (WT) and (B) their anthocyanin contents. The content of the WT was used as a reference and was set to 1. (C) Phenotypes of transient transgenic leaves and the empty vector (EV) and (D) their anthocyanin contents. The content of the EV was used as a reference and was set to 1. All experiments were performed three times with similar results, and representative data from one experiment are shown. Data are means (\pm SD), $n=4$. Different letters indicate significant differences as determined by one-way ANOVA and LSD tests ($P<0.05$). (This figure is available in colour at JXB online.)

such as *DFR* and *UF3GT* (Takos *et al.*, 2006; Ban *et al.*, 2007; Espley *et al.*, 2007; An *et al.*, 2018d, c 2019c, 2020). In our current study, the promotion of anthocyanin accumulation by different light intensities was confirmed in apple fruit and calli (Supplementary Fig. S1). *MdMYB1* was shown to play a key role, as suppression of *MdMYB1* resulted in a significant decrease in the accumulation of anthocyanin in apple calli under different light intensities.

In Arabidopsis, overexpression of *TCP15* decreases anthocyanin biosynthesis and high light inactivates the *TCP15* protein (Viola *et al.*, 2016), whilst *TCP3* plays a positive role in the regulation of biosynthesis by interacting with MYB proteins (Li and Zachgo, 2013). Here, we demonstrated that *MdTCP46* interacted with *MdMYB1* in Y2H, pull-down, and BiFC assays (Fig. 1).

The transcription of *MdTCP46* was stimulated as light intensity increased (Fig. 2B), and the high light treatment dramatically increased the stability of *MdTCP46* (Fig. 2C). This indicates that high light intensity affects the expression of *MdTCP46* at both the transcriptional and post-transcriptional levels. We found that *MdTCP46* positively regulated anthocyanin accumulation in response to different light intensities by up-regulating the expression of biosynthesis genes (Fig. 2D–I; Fig. 3). Overexpression of *MdTCP46* did not interfere with *MdMYB1* expression (Fig. 2F, 3C), which prompted us to examine whether *MdTCP46* affected the binding activity of *MdMYB1* to its target genes. Previous reports have indicated that *MdMYB1* is able to bind to the promoter fragments of

DFR and *UF3GT* (Takos *et al.*, 2006; Ban *et al.*, 2007; Espley *et al.*, 2007; An *et al.*, 2018d, 2019c, 2020). As expected, we found that interaction with *MdTCP46* did indeed facilitate the binding activity of *MdMYB1* to its target genes (Fig. 4C–G), providing evidence that this interaction contributes to anthocyanin biosynthesis induced by high light. Combining our results with those of previous studies, it appears that *MdMYB1* integrates the accumulation of anthocyanin in response to multiple stresses by interacting with different hormones and environmental signal-response factors, such as the ABA-response factor *MdbZIP44*, the wounding-response factor *MdWRKY40*, the drought-response factor *MdERF38*, and the light-response factor *MdTCP46* (Takos *et al.*, 2006; Ban *et al.*, 2007; Espley *et al.*, 2007; An *et al.*, 2018d, 2019c, 2020; Fig. 9B), in each of which *MdMYB1* plays a core regulatory role. Therefore, it seems likely that there may be functional redundancy in these different response factors.

In Arabidopsis, *AtTCP15* is a repressor of anthocyanin biosynthesis and may act by inducing the expression of a PAP1 repressor and other anthocyanin regulatory genes (Viola *et al.*, 2016). Although *MdTCP46* is a *TCP15*-like protein, it exhibits a different function to *AtTCP15* as it is a positive regulator of anthocyanin biosynthesis and is involved in regulating synthesis by interacting with the MBW complex (Viola *et al.*, 2016). Thus species differences in function may exist.

To date, the transcriptional and post-transcriptional regulation of *TCP* proteins have rarely been investigated. Several reports have showed that *TCP* proteins may be regulated by

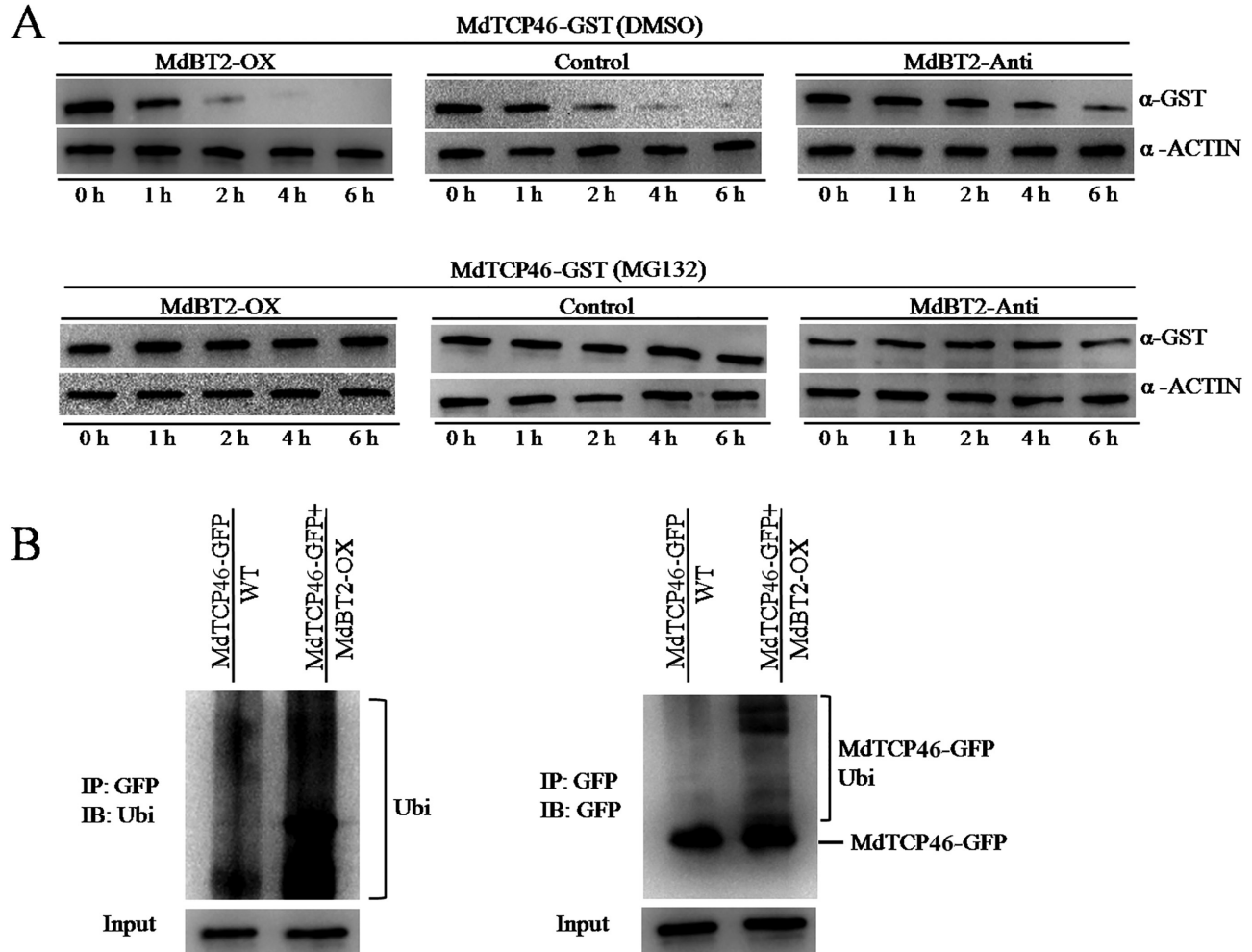


Fig. 8. Mdbt2 degrades the MdTCP46 protein. (A) Detection of MdTCP46-GST fusion proteins in stability assays. Protein extracts were taken from 15-d-old calli grown under dark conditions for the wild-type (WT) and transgenic lines of *Mdbt2*-overexpression (-OX) and *Mdbt2*-antisense (-Anti) and were treated for 0.5 h with either 100 μ M of the proteasome inhibitor MG132 dissolved in DMSO or in DMSO alone (blank control), before being incubated with MdTCP46-GST protein for 0–6 h. ACTIN was used as an internal reference. (B) Mdbt2 promotes the ubiquitination of the MdTCP46 protein *in vivo*. MdTCP46-GFP was immunoprecipitated using the GFP antibody from the two transgenic calli *MdTCP46-GFP* and *MdTCP46-GFP/Mdbt2-OX*. The immunoprecipitated proteins were examined using antibodies for ubiquitin (left) and GFP (right).

miR319 (Schommer et al., 2014; Bresso et al., 2018; Palatnik and Weigel, 2019, Preprint). Since our high light intensity treatment improved the stability of the MdTCP46 protein (Fig. 2C), we examined interacting partners that might have potential roles in regulating this stability. The BTB protein Mdbt2 was found to interact with MdTCP46 (Fig. 5). The expression of *Mdbt2* was inhibited as light intensity increased at both the transcriptional and post-transcriptional levels (Fig. 6C, D), which contrasted with the response pattern of MdTCP46 (Fig. 2B, C). We found that Mdbt2 negatively regulated the biosynthesis of anthocyanin under high light intensity by degrading the MdTCP46 protein directly (Figs 7, 8). Based on these findings, we propose that Mdbt2 mainly functions under low light conditions while high light intensity triggers the accumulation of MdTCP46, which is probably due to the degradation of Mdbt2 that is promoted by high light.

A proposed model that summarizes the functioning of MdTCP46 in light-induced anthocyanin biosynthesis is shown in Fig. 9A. MdTCP46 improves the binding activity of

MdMYB1 to the promoters of *MdDFR* and *MdUF3GT* by directly interacting with it, and thereby promotes the biosynthesis of anthocyanin that is induced by high light. Under low light intensity, Mdbt2 ubiquitinates and degrades the MdTCP46 and MdMYB1 proteins, thus decreasing MdTCP46-promoted accumulation of anthocyanin. As light intensity increases, the expression of *Mdbt2* is inhibited while that of *MdTCP46* is activated, thereby triggering high light intensity-induced anthocyanin biosynthesis. Thus, we speculate that Mdbt2 may act as a dose-responder of light intensity. Our discovery of this ‘Mdbt2–MdTCP46’ ubiquitination regulation module provides new insights that should aid future studies on the post-transcriptional regulation of TCP proteins.

BT2 is a key component of the BT2-CUL3-RBX1 ubiquitin ligase complex, and multiple proteins have been confirmed to be targets for ubiquitination by BT2 (Figueroa et al., 2005; Mandadi et al., 2009; Zhao et al., 2016; An et al., 2018a; Wang et al., 2018). In addition to MdTCP46, different types of Mdbt2-interacting proteins have been identified,

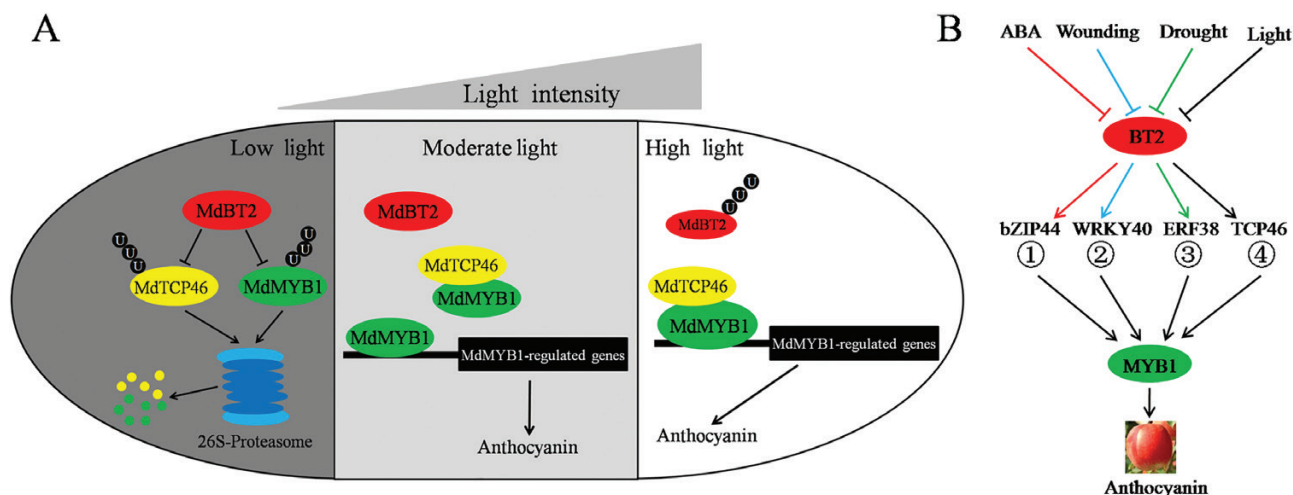


Fig. 9. Proposed model of the functioning of MdTCP46 in light-induced anthocyanin biosynthesis. (A) MdTCP46 interacts with MdMYB1 to increase its transcriptional activity and to enhance its binding to target genes, thereby promoting light-mediated anthocyanin biosynthesis. Under low light, MdBT2 interacts with MdTCP46 to ubiquitinate and degrade it, thus negatively regulating MdTCP46-promoted anthocyanin biosynthesis. Under high light, the transcription of *MdTCP46* is up-regulated and anthocyanin biosynthesis is stimulated. Light inhibits *MdBT2* expression, which in turn releases the MdBT2-enhanced degradation of the MdTCP46 protein, thereby contributing to light-induced anthocyanin biosynthesis. (B) The central role of MdBT2 in anthocyanin biosynthesis mediated by multiple stresses. (1) An *et al.* (2018d); (2) An *et al.* (2019c); (3) An *et al.* (2020); (4) present study. (This figure is available in colour at *JXB* online.)

including MdMYB1, MdMYB9, MdMYB23, MdbHLH93, MdbHLH104, MdBBX22, MdbZIP44, MdWRKY40, and MdERF38 (Zhao *et al.*, 2016; An *et al.*, 2018a, 2018b, 2018d, 2019a, 2019b, 2019c, 2020; Wang *et al.*, 2018). MdBT2 regulates the stability of these proteins through direct interactions and participates in multiple stress-response processes, suggesting that it may be a multifunctional fine-tuning protein that integrates a post-transcriptional regulatory network in response to multiple stress signals. The observations that different transcription factors function as the interaction proteins of both MdBT2 and MdMYB1 indicate that the ‘BT2-interacting proteins–MYB1’ module may be a central component of anthocyanin biosynthesis induced by multiple stresses (Fig. 9B).

Supplementary data

Supplementary data are available at *JXB* online.

Fig. S1. Mediation of anthocyanin biosynthesis at different light intensities is dependent on MdMYB1.

Fig. S2. Identification of transgenic plant material by qRT-PCR.

Fig. S3. Protein sequence alignment of TCP proteins in apple and *Arabidopsis*.

Fig. S4. Yeast two-hybrid assays showing that MdTCP46 specifically interacts with MdMYB1 and MdBT2.

Table S1. The promoter sequence of *MdDFR*.

Table S2. The promoter sequence of *MdUF3GT*.

Table S3. Primers used for gene expression analysis and vector construction.

Acknowledgements

This work was financially supported by grants from the Ministry of Science and Technology of China (2018YFD1000200), the Natural Science

Foundation of China (31772288), the Shandong Province Government (SDAIT-06-03), the Natural Science Foundation of Shandong Province (ZR2019PC004), and the Ministry of Agriculture of China (CARS-27).

References

- Aggarwal P, Das Gupta M, Joseph AP, Chatterjee N, Srinivasan N, Nath U. 2010. Identification of specific DNA binding residues in the TCP family of transcription factors in *Arabidopsis*. *The Plant Cell* **22**, 1174–1189.
- An JP, An XH, Yao JF, Wang XN, You CX, Wang XF, Hao YJ. 2018a. BTB protein MdBT2 inhibits anthocyanin and proanthocyanidin biosynthesis by triggering MdMYB9 degradation in apple. *Tree Physiology* **38**, 1578–1587.
- An JP, Li R, Qu FJ, You CX, Wang XF, Hao YJ. 2018b. R2R3-MYB transcription factor MdMYB23 is involved in the cold tolerance and proanthocyanidin accumulation in apple. *The Plant Journal* **96**, 562–577.
- An JP, Wang XF, Li YY, Song LQ, Zhao LL, You CX, Hao YJ. 2018c. EIN3-LIKE1, MYB1, and ETHYLENE RESPONSE FACTOR3 act in a regulatory loop that synergistically modulates ethylene biosynthesis and anthocyanin accumulation. *Plant Physiology* **178**, 808–823.
- An JP, Wang XF, Zhang XW, Bi SQ, You CX, Hao YJ. 2019a. MdBBX22 regulates UV-B-induced anthocyanin biosynthesis through regulating the function of MdHY5 and is targeted by MdBT2 for 26S proteasome-mediated degradation. *Plant Biotechnology Journal* **17**, 2231–2233.
- An JP, Yao JF, Xu RR, You CX, Wang XF, Hao YJ. 2018d. Apple bZIP transcription factor MdbZIP44 regulates abscisic acid-promoted anthocyanin accumulation. *Plant, Cell & Environment* **41**, 2678–2692.
- An JP, Zhang XW, Bi SQ, You CX, Wang XF, Hao YJ. 2019b. MdbHLH93, an apple activator regulating leaf senescence, is regulated by ABA and MdBT2 in antagonistic ways. *New Phytologist* **222**, 735–751.
- An JP, Zhang XW, Bi SQ, You CX, Wang XF, Hao YJ. 2020. The ERF transcription factor MdERF38 promotes drought stress-induced anthocyanin biosynthesis in apple. *The Plant Journal* **101**, 573–589.
- An JP, Zhang XW, You CX, Bi SQ, Wang XF, Hao YJ. 2019c. MdWRKY40 promotes wounding-induced anthocyanin biosynthesis in association with MdMYB1 and undergoes MdBT2-mediated degradation. *New Phytologist* **224**, 380–395.
- Azuma A, Yakushiji H, Koshita Y, Kobayashi S. 2012. Flavonoid biosynthesis-related genes in grape skin are differentially regulated by temperature and light conditions. *Planta* **236**, 1067–1080.
- Ban Y, Honda C, Hatsuyama Y, Igarashi M, Bessho H, Moriguchi T. 2007. Isolation and functional analysis of a MYB transcription factor gene

that is a key regulator for the development of red coloration in apple skin. *Plant & Cell Physiology* **48**, 958–970.

Braun N, de Saint Germain A, Pillot JP, et al. 2012. The pea TCP transcription factor PsBRC1 acts downstream of strigolactones to control shoot branching. *Plant Physiology* **158**, 225–238.

Bresso EG, Chorostecki U, Rodriguez RE, Palatnik JF, Schommer C. 2018. Spatial control of gene expression by miR319-regulated TCP transcription factors in leaf development. *Plant Physiology* **176**, 1694–1708.

Busch A, Deckena M, Almeida-Trapp M, Kopischke S, Kock C, Schüssler E, Tsiantis M, Mithöfer A, Zachgo S. 2019. MpTCP1 controls cell proliferation and redox processes in *Marchantia polymorpha*. *New Phytologist* **224**, 1627–1641.

Carbone F, Preuss A, De Vos RC, D'Amico E, Perrotta G, Bovy AG, Martens S, Rosati C. 2009. Developmental, genetic and environmental factors affect the expression of flavonoid genes, enzymes and metabolites in strawberry fruits. *Plant, Cell & Environment* **32**, 1117–1131.

Chahel AA, Zeng S, Yousaf Z, Liao Y, Yang Z, Wei X, Ying W. 2019. Plant-specific transcription factor LrTCP4 enhances secondary metabolite biosynthesis in *Lycium ruthenicum* hairy roots. *Plant Cell, Tissue and Organ Culture* **136**, 323–337.

Clough SJ, Bent AF. 1998. Floral dip: a simplified method for *Agrobacterium*-mediated transformation of *Arabidopsis thaliana*. *The Plant Journal* **16**, 735–743.

Corley SB, Carpenter R, Copsey L, Coen E. 2005. Floral asymmetry involves an interplay between TCP and MYB transcription factors in *Antirrhinum*. *Proceedings of the National Academy of Sciences, USA* **102**, 5068–5073.

Cubas P, Lauter N, Doebley J, Coen E. 1999. The TCP domain: a motif found in proteins regulating plant growth and development. *The Plant Journal* **18**, 215–222.

Danisman S, van der Wal F, Dhondt S, et al. 2012. *Arabidopsis* class I and class II TCP transcription factors regulate jasmonic acid metabolism and leaf development antagonistically. *Plant Physiology* **159**, 1511–1523.

Espley RV, Hellens RP, Putterill J, Stevenson DE, Kutty-Amma S, Allan AC. 2007. Red colouration in apple fruit is due to the activity of the MYB transcription factor, MdMYB10. *The Plant Journal* **49**, 414–427.

Fang H, Dong Y, Yue X, et al. 2019. The B-box zinc finger protein MdBBX20 integrates anthocyanin accumulation in response to ultraviolet radiation and low temperature. *Plant, Cell & Environment* **42**, 2090–2104.

Figuroa P, Gusmaroli G, Serino G, et al. 2005. *Arabidopsis* has two redundant Cullin3 proteins that are essential for embryo development and that interact with RBX1 and BTB proteins to form multisubunit E3 ubiquitin ligase complexes *in vivo*. *The Plant Cell* **17**, 1180–1195.

Gong D, Cao S, Sheng T, Shao J, Song C, Wo F, Chen W, Yang Z. 2015. Effect of blue light on ethylene biosynthesis, signalling and fruit ripening in postharvest peaches. *Scientia Horticulturae* **197**, 657–664.

Guan L, Dai Z, Wu BH, et al. 2016. Anthocyanin biosynthesis is differentially regulated by light in the skin and flesh of white-fleshed and teinturier grape berries. *Planta* **243**, 23–41.

Guo Z, Fujioka S, Blancaflor EB, Miao S, Gou X, Li J. 2010. TCP1 modulates brassinosteroid biosynthesis by regulating the expression of the key biosynthetic gene *DWARF4* in *Arabidopsis thaliana*. *The Plant Cell* **22**, 1161–1173.

Henry-Kirk RA, Plunkett B, Hall M, McGhie T, Allan AC, Wargent JJ, Espley RV. 2018. Solar UV light regulates flavonoid metabolism in apple (*Malus × domestica*). *Plant, Cell & Environment* **41**, 675–688.

Hichri I, Barrieu F, Bogs J, Kappel C, Delrot S, Lauvegeat V. 2011. Recent advances in the transcriptional regulation of the flavonoid biosynthetic pathway. *Journal of Experimental Botany* **62**, 2465–2483.

Honda C, Moriya S. 2018. Anthocyanin biosynthesis in apple fruit. *Horticulture Journal* **87**, 305–314.

Jaakola L. 2013. New insights into the regulation of anthocyanin biosynthesis in fruits. *Trends in Plant Science* **18**, 477–483.

Jiang M, Ren L, Lian H, Liu Y, Chen H. 2016. Novel insight into the mechanism underlying light-controlled anthocyanin accumulation in eggplant (*Solanum melongena* L.). *Plant Science* **249**, 46–58.

Kieffer M, Master V, Waites R, Davies B. 2011. TCP14 and TCP15 affect internode length and leaf shape in *Arabidopsis*. *The Plant Journal* **68**, 147–158.

Koyama T, Mitsuda N, Seki M, Shinozaki K, Ohme-Takagi M. 2010. TCP transcription factors regulate the activities of ASYMMETRIC LEAVES1 and miR164, as well as the auxin response, during differentiation of leaves in *Arabidopsis*. *The Plant Cell* **22**, 3574–3588.

Li S, Zachgo S. 2013. TCP3 interacts with R2R3-MYB proteins, promotes flavonoid biosynthesis and negatively regulates the auxin response in *Arabidopsis thaliana*. *The Plant Journal* **76**, 901–913.

Li YY, Mao K, Zhao C, Zhao XY, Zhang HL, Shu HR, Hao YJ. 2012. MdCOP1 ubiquitin E3 ligases interact with MdMYB1 to regulate light-induced anthocyanin biosynthesis and red fruit coloration in apple. *Plant Physiology* **160**, 1011–1022.

Lin-Wang K, Bolitho K, Grafton K, Kortstee A, Karunairetnam S, McGhie TK, Espley RV, Hellens RP, Allan AC. 2010. An R2R3 MYB transcription factor associated with regulation of the anthocyanin biosynthetic pathway in *Rosaceae*. *BMC Plant Biology* **10**, 50.

Ma YN, Xu DB, Li L, et al. 2018. Jasmonate promotes artemisinin biosynthesis by activating the TCP14-ORA complex in *Artemisia annua*. *Science Advances* **4**, eaas9357.

Manassero NGU, Viola IL, Welchen E, Gonzalez DH. 2013. TCP transcription factors: architectures of plant form. *Biomolecular Concepts* **4**, 111–127.

Mandadi KK, Misra A, Ren S, McKnight TD. 2009. BT2, a BTB protein, mediates multiple responses to nutrients, stresses, and hormones in *Arabidopsis*. *Plant Physiology* **150**, 1930–1939.

Martín-Trillo M, Cubas P. 2010. TCP genes: a family snapshot ten years later. *Trends in Plant Science* **15**, 31–39.

Meng X, Xing T, Wang X. 2004. The role of light in the regulation of anthocyanin accumulation in *Gerbera hybrida*. *Plant Growth Regulation* **44**, 243.

Min L, Hu Q, Li Y, Xu J, Ma Y, Zhu L, Yang X, Zhang X. 2015. LEAFY COTYLEDON1-CASEIN KINASE I-TCP15-PHYTOCHROME INTERACTING FACTOR4 network regulates somatic embryogenesis by regulating auxin homeostasis. *Plant Physiology* **169**, 2805–2821.

Mukhopadhyay P, Tyagi AK. 2015. *OsTCP19* influences developmental and abiotic stress signaling by modulating ABI4-mediated pathways. *Scientific Reports* **5**, 9998.

Ni J, Bai S, Zhao Y, Qian M, Tao R, Yin L, Gao L, Teng Y. 2019. Ethylene response factors Pp4ERF24 and Pp12ERF96 regulate blue light-induced anthocyanin biosynthesis in 'Red Zaosu' pear fruits by interacting with MYB114. *Plant Molecular Biology* **99**, 67–78.

Nicolas M, Cubas P. 2016. TCP factors: new kids on the signaling block. *Current Opinion in Plant Biology* **33**, 33–41.

Niu SS, Xu CJ, Zhang WS, Zhang B, Li X, Lin-Wang K, Ferguson IB, Allan AC, Chen KS. 2010. Coordinated regulation of anthocyanin biosynthesis in Chinese bayberry (*Myrica rubra*) fruit by a R2R3 MYB transcription factor. *Planta* **231**, 887–899.

Ordidge M, García-Macías P, Battey NH, Gordon MH, John P, Lovegrove JA, Vysini E, Wagstaffe A, Hadley P. 2012. Development of colour and firmness in strawberry crops is UV light sensitive, but colour is not a good predictor of several quality parameters. *Journal of the Science of Food and Agriculture* **92**, 1597–1604.

Palatnik JF, Weigel D. 2019. Specific regulation of TCP genes by miR319. *bioRxiv* 747790. [Preprint].

Pruneda-Paz JL, Kay SA. 2010. An expanding universe of circadian networks in higher plants. *Trends in Plant Science* **15**, 259–265.

Sarvepalli K, Nath U. 2011. Hyper-activation of the TCP4 transcription factor in *Arabidopsis thaliana* accelerates multiple aspects of plant maturation. *The Plant Journal* **67**, 595–607.

Schommer C, Debernardi JM, Bresso EG, Rodriguez RE, Palatnik JF. 2014. Repression of cell proliferation by miR319-regulated TCP4. *Molecular Plant* **7**, 1533–1544.

Schwinn KE, Ngo H, Kenel F, Brummell DA, Albert NW, McCallum JA, Pither-Joyce M, Crowhurst RN, Eady C, Davies KM. 2016. The onion (*Allium cepa* L.) R2R3-MYB gene *MYB1* regulates anthocyanin biosynthesis. *Frontiers in Plant Science* **7**, 1865.

Takos AM, Jaffé FW, Jacob SR, Bogs J, Robinson SP, Walker AR. 2006. Light-induced expression of a *MYB* gene regulates anthocyanin biosynthesis in red apples. *Plant Physiology* **142**, 1216–1232.

Tao R, Bai S, Ni J, Yang Q, Zhao Y, Teng Y. 2018. The blue light signal transduction pathway is involved in anthocyanin accumulation in 'Red Zaosu' pear. *Planta* **248**, 37–48.

- Tatematsu K, Nakabayashi K, Kamiya Y, Nambara E.** 2008. Transcription factor AtTCP14 regulates embryonic growth potential during seed germination in *Arabidopsis thaliana*. *The Plant Journal* **53**, 42–52.
- Telias A, Lin-Wang K, Stevenson DE, Cooney JM, Hellens RP, Allan AC, Hoover EE, Bradeen JM.** 2011. Apple skin patterning is associated with differential expression of *MYB10*. *BMC Plant Biology* **11**, 93.
- Trojak M, Skowron E.** 2017. Role of anthocyanins in high-light stress response. *World Scientific News* **81**, 150–168.
- Ubi BE, Honda C, Bessho H, Kondo S, Wada M, Kobayashi S, Moriguchi T.** 2006. Expression analysis of anthocyanin biosynthetic genes in apple skin: effect of UV-B and temperature. *Plant Science* **170**, 571–578.
- Viola IL, Camoirano A, Gonzalez DH.** 2016. Redox-dependent modulation of anthocyanin biosynthesis by the TCP transcription factor TCP15 during exposure to high light intensity conditions in *Arabidopsis*. *Plant Physiology* **170**, 74–85.
- Wang XF, An JP, Liu X, Su L, You CX, Hao YJ.** 2018. The nitrate-responsive protein MdBT2 regulates anthocyanin biosynthesis by interacting with the MdMYB1 transcription factor. *Plant Physiology* **178**, 890–906.
- Weir I, Lu J, Cook H, Causier B, Schwarz-Sommer Z, Davies B.** 2004. *CUPULIFORMIS* establishes lateral organ boundaries in *Antirrhinum*. *Development* **131**, 915–922.
- Winkel-Shirley B.** 1999. Evidence for enzyme complexes in the phenylpropanoid and flavonoid pathways. *Physiologia Plantarum* **107**, 142–149.
- Winkel-Shirley B.** 2001. Flavonoid biosynthesis. A colorful model for genetics, biochemistry, cell biology, and biotechnology. *Plant Physiology* **126**, 485–493.
- Winkel-Shirley B.** 2002. Biosynthesis of flavonoids and effects of stress. *Current Opinion in Plant Biology* **5**, 218–223.
- Xie X, Zhao J, Hao YJ, Fang C, Wang Y.** 2017. The ectopic expression of apple *MYB1* and *bHLH3* differentially activates anthocyanin biosynthesis in tobacco. *Plant Cell, Tissue and Organ Culture* **131**, 183–194.
- Xu R, Sun P, Jia F, Lu L, Li Y, Zhang S, Huang J.** 2014. Genomewide analysis of *TCP* transcription factor gene family in *Malus domestica*. *Journal of Genetics* **93**, 733–746.
- Yao X, Ma H, Wang J, Zhang D.** 2007. Genome-wide comparative analysis and expression pattern of TCP gene families in *Arabidopsis thaliana* and *Oryza sativa*. *Journal of Integrative Plant Biology* **49**, 885–897.
- Yi G, Kim JS, Park JE, Shin H, Yu SH, Park S, Huh JH.** 2018. MYB1 transcription factor is a candidate responsible for red root skin in radish (*Raphanus sativus* L.). *PLoS ONE* **13**, e0204241.
- Zhang Y, Jiang L, Li Y, Chen Q, Ye Y, Zhang Y, Luo Y, Sun B, Wang X, Tang H.** 2018a. Effect of red and blue light on anthocyanin accumulation and differential gene expression in strawberry (*Fragaria × ananassa*). *Molecules* **23**, 820.
- Zhang Y, Xu S, Cheng Y, Peng Z, Han J.** 2018b. Transcriptome profiling of anthocyanin-related genes reveals effects of light intensity on anthocyanin biosynthesis in red leaf lettuce. *PeerJ* **6**, e4607.
- Zhao Q, Ren YR, Wang QJ, Wang XF, You CX, Hao YJ.** 2016. Ubiquitination-related MdBT scaffold proteins target a bHLH transcription factor for iron homeostasis. *Plant Physiology* **172**, 1973–1988.
- Zoratti L, Karppinen K, Luengo Escobar A, Häggman H, Jaakola L.** 2014. Light-controlled flavonoid biosynthesis in fruits. *Frontiers in Plant Science* **5**, 534.